



Vrije Universiteit Brussel

Faculteit Geneeskunde en Farmacie  
Vrije Universiteit Brussel  
Laarbeeklaan 103  
B-1090 Brussel

**ENU mutagenesis as a discovery and validation tool of potential driver genes in pancreatic tumourigenesis**

**Mathias Van Bulck**

Eindwerk, ingediend voor het behalen van de graad van Master in de Biomedische Wetenschappen

16 augustus 2013  
Academiejaar 2012 – 2013

Promotor: Prof. Dr. Ilse Rooman

Begeleider: Amanda Mawson , Dr. Andreia V. Pinho,  
Dr. Marc Giry-Laterrière

Naam en adres van de stageplaats  
The Kinghorn Cancer Centre,  
The Garvan Institute of Medical Research,  
384 Victoria street, 2010 Darlinghurst,  
Sydney, Australia



**1. Table of contents**

<b>1. Table of contents</b> .....	<b>2</b>
<b>2. Summary/abstract</b> .....	<b>4</b>
<b>2bis. Samenvatting</b> .....	<b>5</b>
<b>3. Introduction</b> .....	<b>6</b>
3.1. Pancreatic ductal adenocarcinoma (PDAC) .....	6
3.1.1. <i>Prevalence, risk and therapy</i> .....	6
3.1.2. <i>Precursor lesions: the beginning of the end</i> .....	6
3.1.3. <i>in vitro assay of acinar to ductal metaplasia</i> .....	9
3.1.4. <i>Mouse models of PDAC</i> .....	10
3.1.5. <i>The 'International Cancer Genome Consortium': a catalogue of potential drivers</i> .....	10
3.2. ENU mutagenesis: going forward or reverse.....	12
3.3. Study aim and workflow .....	13
<b>4. Material and methods</b> .....	<b>14</b>
4.1. ENU-mutant mouse generation.....	14
4.2. Acinar cell isolation and culture .....	14
4.2.1. <i>Animals</i> .....	14
4.2.2. <i>ADM assay</i> .....	14
4.3. Cell lines and inducible expression systems.....	14
4.3.1. <i>Overexpression construct</i> .....	14
4.3.2. <i>Knockdown construct</i> .....	15
4.3.3. <i>Virus production</i> .....	15
4.3.4. <i>Transduction of 266-6 mouse pancreatic acinar cell line</i> .....	15
4.4. Immunostainings .....	15
4.4.1. <i>Immunohistochemistry (IHC)</i> .....	15
4.4.2. <i>Proliferation quantification</i> .....	16

---

4.4.3. Immunofluorescence (IF) .....	16
4.5. Real-time reverse transcription polymerase chain reaction (RT-qPCR) .....	16
4.6. One-dimensional sodium dodecyl sulfate polyacrylamide gel electrophoresis (SDS-Page) and Western Blot .....	17
4.6.1. Densitometric quantification.....	17
4.7. Antibodies .....	18
4.8. Protein structure prediction.....	18
4.9. Statistical analyses .....	18
<b>5. Results .....</b>	<b>19</b>
5.1. Driver gene discovery approach .....	19
5.1.1. Phenotype presentation and causative mutation determination .....	19
5.1.2. Hit discovery and analysis .....	23
5.1.3. <i>GUCD1</i> mRNA expression analysis.....	24
5.1.4. Overexpression assessment of <i>GUCD1</i> -HA transduced 266-6 mouse pancreatic acinar cell line .....	25
5.1.5. ADM assay of homozygous <i>Gucd1</i> mutant mice .....	27
5.2. Validation approach of Timeless as potential driver gene in pancreatic tumourigenesis using ENU mutagenesis .....	28
5.2.1. Timeless protein expression in the pancreas of heterozygous <i>Tim</i> mutant mice .....	28
5.2.2. <i>in vitro</i> ADM assay and whole pancreas analysis .....	28
<b>6. Discussion.....</b>	<b>30</b>
<b>7. References .....</b>	<b>33</b>
<b>8. Abbreviations .....</b>	<b>37</b>
<b>9. Acknowledgements and CV .....</b>	<b>40</b>

## 2. Summary/abstract

Pancreatic ductal adenocarcinoma (PDAC), the most common form of pancreatic cancer, has a poor outcome with a median survival of less than 6 months. Early detection and better treatment requires fundamental insights into tumour initiation and early progression. Recent evidence from mouse models of PDAC show that ductal-type tumours can arise from acinar cells through a mechanism called acinar to ductal metaplasia (ADM). Discovering the genes that play a role in ADM, initiate preneoplastic conditions and contribute to tumour progression could pinpoint potential leads for novel detection and/or treatment strategies.

We used N-ethyl-N-nitrosourea (ENU) mutagenesis as the basis to discover and validate genes potentially involved in ADM and PDAC initiation. We complemented our data with results from exome sequencing and transcriptomic analysis of patient tumour samples.

We used a forward ENU mutagenesis screen to assess the progeny of ENU-mutated mice for ADM and increased proliferation in the pancreatic exocrine tissue. Potential causative genes were discovered by next generation sequencing (NGS) of the affected mice. Further examination of the affected pedigree correlated the phenotype with a homozygous non-synonymous missense mutation in the uncharacterized gene *Gucd1* (Guanylyl cyclase-containing domain 1). Mutations were located in a highly conserved functionally annotated domain, and found ‘possibly damaging’ by computational prediction methods. Examination of ADM in a specific *in vitro* assay using pancreatic cells from the homozygous *Gucd1* mutant mice showed higher *Gucd1* expression, as well as a more pronounced ADM with a downregulation of the acinar transcription factor *Ptf1a* and enzyme *Amy2* and an upregulation of *Sox9*, a ductal gene highly implicated in ADM and PDAC development. *GUCD1* expression in patient tumours tends to inversely correlate with survival outcomes. Seemingly in contrast, mRNA expression analysis for *Gucd1* showed a significant decrease in mouse models of pancreatic tumourigenesis versus normal tissue. Overexpression of full length *GUCD1* in 266-6 mouse acinar cells had no consistent effects on ADM. Altogether we have identified a so far uncharacterised gene with an apparent role in pancreatic ADM that is worth to be investigated further.

In a second part of this thesis, we used mice with an ENU-induced mutation in the circadian gene *TIMELESS (TIM)*. Our data showed genetic aberrations in the *TIM* gene to be present in around 10% of pancreatic tumours. Pancreatic cells from the mutant *Tim* mice were analysed using the ADM assay but did not display altered ADM related gene expression, except for an increase in *Sox9*. These preliminary results suggest that *Tim* is not overtly implicated in ADM though can still play a role in the established tumour.

In conclusion, we successfully used ENU mutagenesis for the study of pancreatic cancer. Both the discovery (*GUCD1*) and validation (*TIMELESS*) approach now require functional analyses to further define the gene function associated with ADM or tumour progression respectively for *GUCD1* and *TIM*.

### 3. Introduction

#### 3.1. Pancreatic ductal adenocarcinoma (PDAC)

##### 3.1.1. Prevalence, risk and therapy.

Pancreatic Ductal Adenocarcinoma (PDAC), the most common form of exocrine pancreas cancer is a leading cause of cancer death (1) (Figure 1) . Patients face a 5-year survival rate of less than 5% after diagnosis (2). If detected at early stage, outcomes are considerably improved. The occurrence of pancreatic cancer is rare before the age of 40 and median age of diagnosis is around 70 years (1).

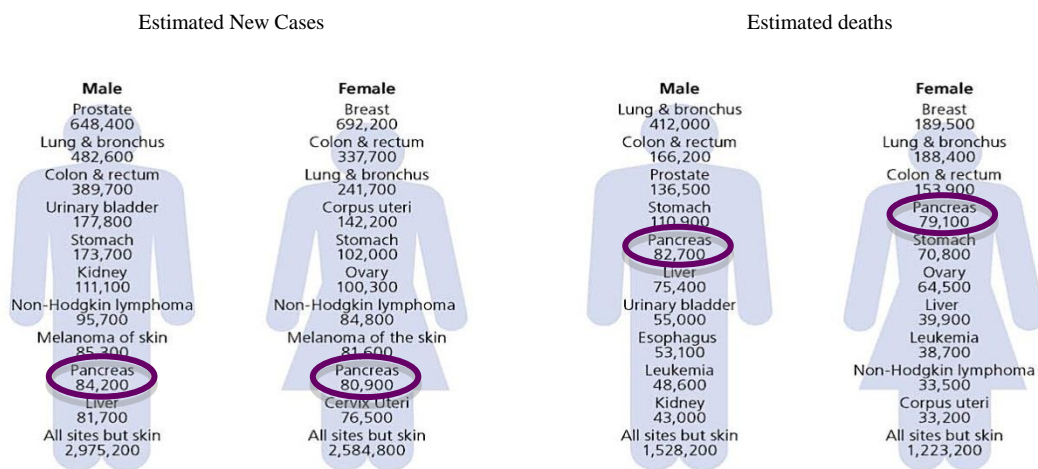


Figure 1. Estimated new cancer cases and deaths in males and females in developed countries (1).

Several risk factors for PDAC have been identified. Cigarette smoking doubles the risk and is by far the leading preventable risk factor. Other established risk factors are family history, obesity, long-standing diabetes mellitus and chronic pancreatitis (3–5).

Pancreatic cancer is characterized by a high propensity for local invasion and distant metastasis as well as a largely drug-resistant phenotype (2). Standard of care since 1997 includes gemcitabine-based regimens (6).

##### 3.1.2. Precursor lesions: the beginning of the end.

Invasive PDAC is believed to arise from a spectrum of preneoplastic mucinous lesions with ductal morphology, i.e. pancreatic intra-epithelial neoplasias (PanINs), mucinous cystic neoplasias (MCNs) and intraductal papillary mucinous neoplasias (IPMNs) (7). PanINs are the most common preneoplastic lesions observed in humans and recent data from mouse models indicate that these lesions can develop from the digestive enzyme secreting acinar cells (Figure 2) through a process of **acinar to ductal metaplasia (ADM)**.

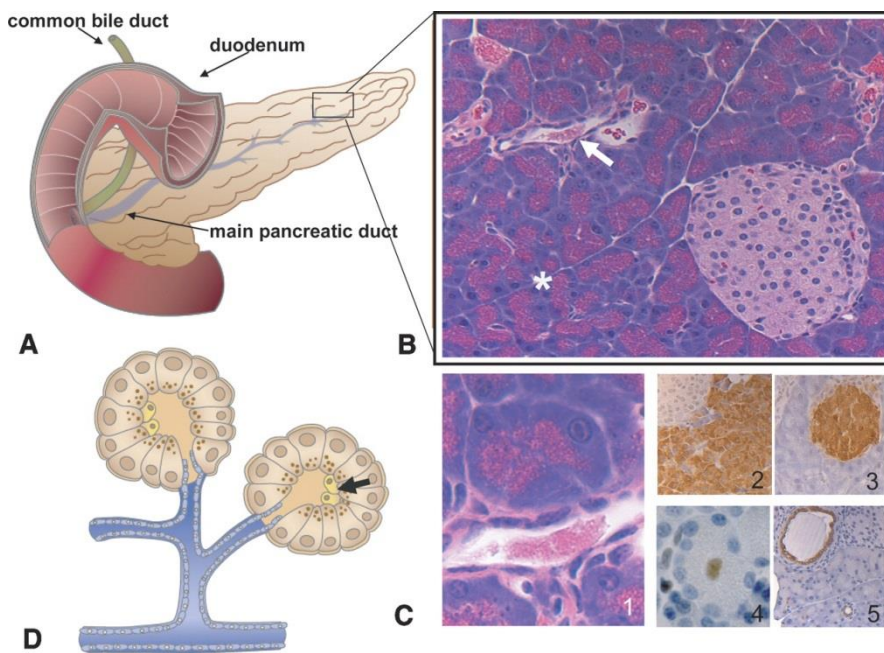


**Figure 2. Anatomy of the pancreas adopted from (7).** The pancreas is comprised of separate functional units belonging to either the exocrine or endocrine portion of the organ, regulating two major physiological processes respectively digestion and glucose metabolism. (A) Overview of the pancreas adjacent to common bile duct and duodenum. (B) The major histological components of the pancreatic parenchyma with lower right an islet of Langerhans, the endocrine portion of the pancreas. The exocrine part is comprised of acini (asterisk) which secrete their zymogens into the ducts (white arrow). H&E stain. (C) H&E and IHC stained sections of various pancreatic cell types. (Panel 1) Acinar cells in relationship to the ducts. (Panel 2) Acinar cells visualized in brown with an antibody against the enzyme amylase 2. (Panel 3) Islet of Langerhans visualized with an antibody against insulin. (Panel 4) A centroacinar cell showing Hes1 staining. (Panel 5) Ductal cells in cross section

ADM is characterized by conversion of acinar cells into cells expressing ductal markers (8,9). ADM is also observed in pancreatitis, which is a major risk factor for PDAC in humans (10). During pancreatic cancer progression, accumulation of genetic mutations in these lesions leads to an increasing degree of atypia and ultimately PDAC (11). The earliest detectable mutations found in preneoplastic lesions of PDAC are activating mutations in the KRAS oncogene (12,13) (Figure 3). These mutations are the single common genetic abnormality in pancreatic cancer being present in about 90-95% of cases (14). KRAS is a member of the RAS family of guanosine triphosphate binding proteins that mediate a range of cellular functions including proliferation, cell survival, cytoskeletal remodelling and motility among others (15). Activated KRAS interacts with a number of downstream effector pathways, including RAF-mitogen-activated-protein-kinase (RAF-MAPK), phosphoinositide-3-kinase (PI3K), and RalGDS pathways.

Mice in which KRAS is activated through mutation develop PanINs and, in some cases to PDAC (16) (Figure 3). ADM, that can be provoked by experimentally induced pancreatitis but also overexpression of the ductal cell fate determinant Sox9, facilitates and accelerates KRAS<sup>G12D</sup>-mediated PanIN and PDAC formation in adult mice (16–19). Sox9 plays an important role in ADM and PanIN formation as loss- and gain-of-function experiments identified the transcription factor as a critical mediator of KRAS-induced premalignant acinar cell reprogramming and inducer of Krt19 expression (ductal marker) (19). As such Sox9 promotes and is required for PanIN formation originating from the acinar cell compartment (19).

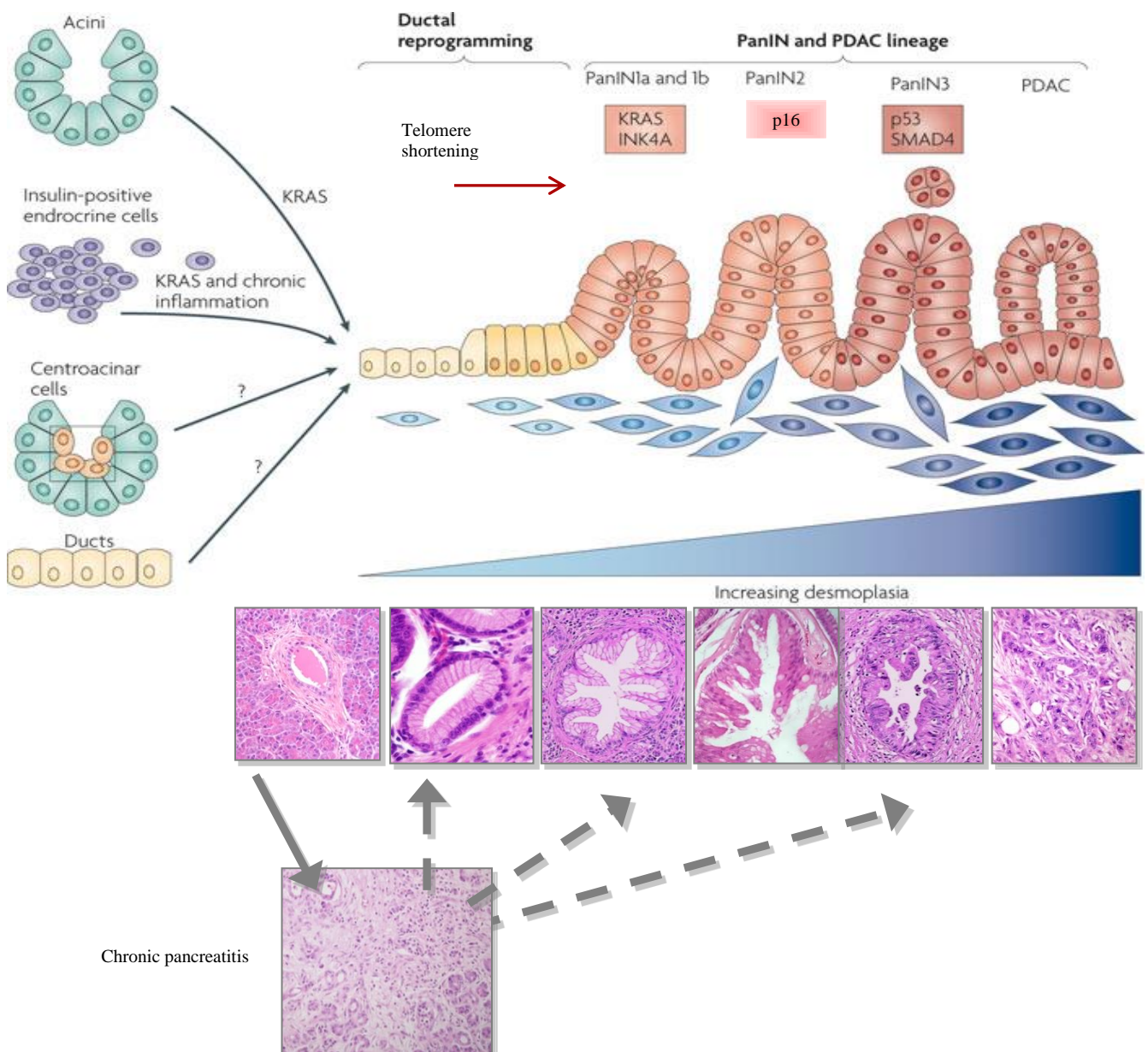


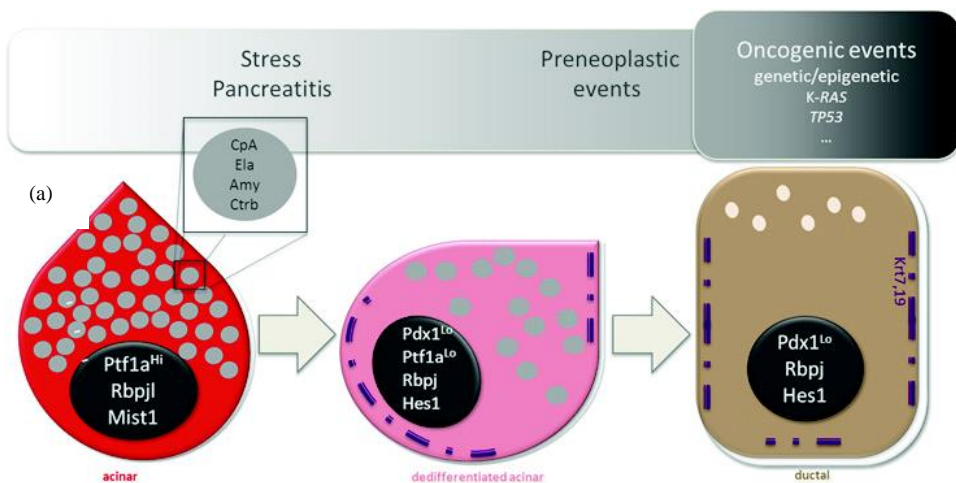
**Figure 3. Acinar to ductal metaplasia and the progression towards malignancy (modified from (14,18)).** Signalling events leading to Kras activation beyond a certain threshold i.e. Kras mutation and pancreatitis may modulate the differentiation state of acinar cells and render them more permissive to malignant transformation (21). Pancreatic tumorigenesis can be classified into early (telomere shortening and activating mutations in KRAS), intermediate (inactivating mutations or epigenetic silencing of p16) and late (inactivating mutations in p53 and SMAD4) events. Constitutively active Kras is sufficient to initiate the development of PanIN and PDAC. PanINs are classified into three stages of increasing cellular atypia and have been found to harbour increasing numbers of mutations. Reprogramming of acinar and possibly also insulin-positive cells into a ‘ductal’ cell type has been demonstrated. Changes in the epithelium are matched by desmoplastic changes in the stroma. Question marks are shown for centroacinar and duct cells as they have not been specifically assessed for this ability and/or lack evidence. H&E stains show the progression in the human pancreas in parallel with the mouse progression model. Chronic pancreatitis is a major risk factor for PDAC and may lead to preneoplastic lesions through acinar to ductal metaplasia (ADM).

3.1.3. *In vitro* assay of acinar to ductal metaplasia

The ADM assay replicates *in vitro* the events occurring in chronic pancreatitis (20). It allows to assay the specific changes in isolated acini that undergo dedifferentiation to a ductal phenotype. Note that adult pancreatic acinar and duct cells have developed from a common embryonic progenitor with ductal characteristics. Few markers distinguish between embryonic and adult duct cells. Depending on the culture conditions in the ADM assay (suspension or monolayer culture), the resulting ductal phenotype is slightly different, with the suspension cultures representing more embryonic ductal features.

Figure 4 adopted from (20,21), shows that rodent acini can be cultured as aggregates and undergo stress similar to pancreatitis. The acinar cells then dedifferentiate into pancreatic progenitor-like cells. From the ADM assay, we have learnt that this implies the downregulation of expression of acinar cell specific transcriptional regulators (high level of Ptf1a expression (Ptf1a<sup>hi</sup>), Rbpjl and Mist1), their target genes that encode for digestive enzymes (e.g. Carboxypeptidase A1 (Cpa1), Elastase 2 (Ela2), Amylase (Amy2) and Chymotrypsin (Ctrb)). The cells in the ADM assay have gained embryonic features such as activation of expression of Hes1, low Pdx (Pdx<sup>lo</sup>) and Ptf1a (Ptf1a<sup>lo</sup>) levels, and Rbpj replaces Rbpjl. Duct cell specific keratins, e.g. Krt7 and Krt19 are induced. In monolayer cultures of these aggregates, Ptf1a and Pdx1 expression are lost, suggestive of a more mature ductal phenotype. The dedifferentiation sensitizes the cells to both genetic (i.e. mutations, allele loss) and epigenetic (methylation, histone modification) changes that promote PDAC development.

**Figure 4.** *in vitro* ADM assay mimics events occurring during chronic pancreatitis. Acinar cells undergoing stress e.g. pancreatitis dedifferentiate and subsequently lose the mature phenotype, as a result dedifferentiated acini obtain embryonic traits. This is an initiating event of pancreatic tumourigenesis.



The ADM assay is ideal for screening genes for a role in pancreatic tumourigenesis because it subjects the acinar cells to the common PDAC initiation event of ADM. It is a fast technique, suitable for high/mid-throughput in comparison with a chronic pancreatitis experiment. In addition, it allows the selective analysis of the epithelial cells as the technique provides a near pure population of acinar cells. At the same time the effects of the immune system, present in a living mouse model of chronic pancreatitis and putatively impacting your results, can be excluded.

### 3.1.4. mouse models of PDAC

The idea of ADM is not new (22,23). This became evident for *Ela1-TGF $\alpha$*  and *Ela1-c-myc* transgenic mice presenting with ADM and development of acinar-derived ductal tumours (24,25). Selective activation of mutant *Kras* in acinar cells and extensive lineage tracing have confirmed the ability of differentiated acinar cells to undergo ADM upon caerulein-induced pancreatitis (15,17).

The significance of *Kras* mutations has been demonstrated in mice, where expression of the constitutively active *Kras*<sup>G12D or G12V</sup> allele induces PanINs and after a significant latency period also PDAC (26). Even after a long latency only 10% of mice develop invasive, metastatic adenocarcinomas. This low frequency of progression to invasive adenocarcinomas is likely a consequence of *Kras*-induced senescence in the preinvasive lesions (26). This underscores the use of cooperating mutations in the *Ink4a-Rb* or *Arf-p53* checkpoint (27,28). We mostly use the KPC mouse model (*Pdx1-Cre; K-Ras*<sup>+/*LSLG12D*</sup>; *p53*<sup>R172H/+</sup>) where the inactivating *p53* mutation, in addition to activated mutant *Kras*, leads to the development of lethal, metastatic pancreatic tumours with complete penetrance and shorter latency thereby recapitulating the progression of human PDAC in mice (29).

### 3.1.5. The 'International Cancer Genome consortium': a catalogue of potential drivers

It is of utmost interest to increase the knowledge on those genes that are aberrantly expressed at the initial stages of PDAC and assess their 'actionability' as screening or intervention targets in early pancreas disease.

The Pancreatic Cancer research group where this thesis was undertaken is part of the 'International Cancer Genome Consortium' (ICGC), which recently sequenced around 100 pancreatic tumours showing the presence of more than 2000 non-silent mutations and 1600 copy number variants (CNVs) (30). New genes and pathways were identified that are possibly important in PDAC development. Therefore, the recent work contributes to a validation process to unravel the driver/founder genes in the onset of pancreatic cancer, with specific attention to ADM.

The next generation sequencing (NGS) data from the PDAC tumours showed that the circadian gene *TIMELESS (TIM)* was mutated in 10% of human pancreatic cancers either through mutation or CNVs. TIM protein expression was assessed by immunohistochemistry in 54 patients. Very high TIM protein expression was found in a patient sample with mutation in the *TIM* gene (D1174N) (Figure 5). Low intensity staining is present in normal pancreas (not shown)

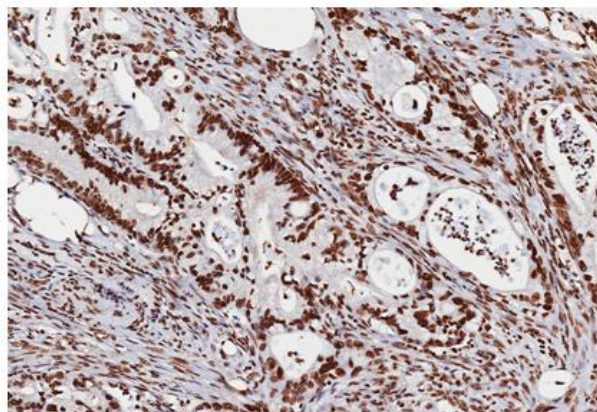


**Figure 5. TIM expression in PDAC.** Strong expression (3+) of TIM in a patient with PDAC.

TIM protein expression in the cohort was used to establish survival rates. Using a 50% expression cut-off, patients with low TIM expression had significantly improved survival ( $p=0,01307$ ; Figure 6.).

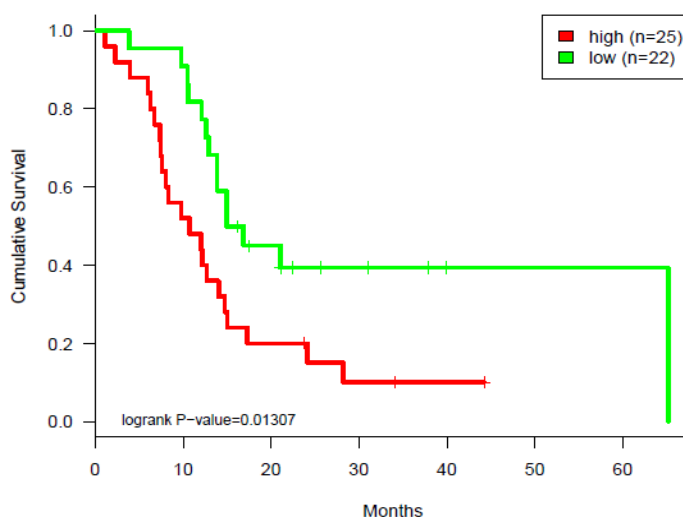


Figure 6. Kaplan-Meier survival curve showing a survival benefit in PDAC patients with low TIM expression.

Together, these data sparked our interest to further validate the importance of Timeless in PDAC development.

TIM has an important role in maintaining and monitoring the integrity of DNA replication forks in eukaryotes and is involved in cell survival after DNA damage or replication stress (37). Furthermore it is required for normal intra S-phase progression (31). Tim was named after the *Drosophila* homolog. *Drosophila* Tim is also involved in the regulation of the circadian rhythm, this resulted in the proposal that there is an intimate association between genome maintenance mechanisms and the control of biological time (32). Evidently failures in DNA replication are a potent force for driving genomic instability (31). Deletion of TIM orthologues leads to an embryonic lethal phenotype in mice and *Caenorhabditis Elegans*, most likely due to its role in DNA replication (33,34).

The oncogenic potential of circadian disruption was supported by evidence from Stevens, Hansen and Davis, reporting female nightshift workers are at increased risk of developing breast cancer (35). TIM may also play an important role in epithelial cell morphogenesis and formation of branching tubules to the daily rhythm of the circadian cycle (37).

TIM and TIPIN (TIM interacting protein) are required for CHK1 phosphorylation and TIM may be specifically required for the ATR-CHK1 pathway in the replication checkpoint induced by hydroxyurea or ultraviolet light (31). Therefore TIM can be an interesting drugable target via existing CHK1 inhibitors (36).

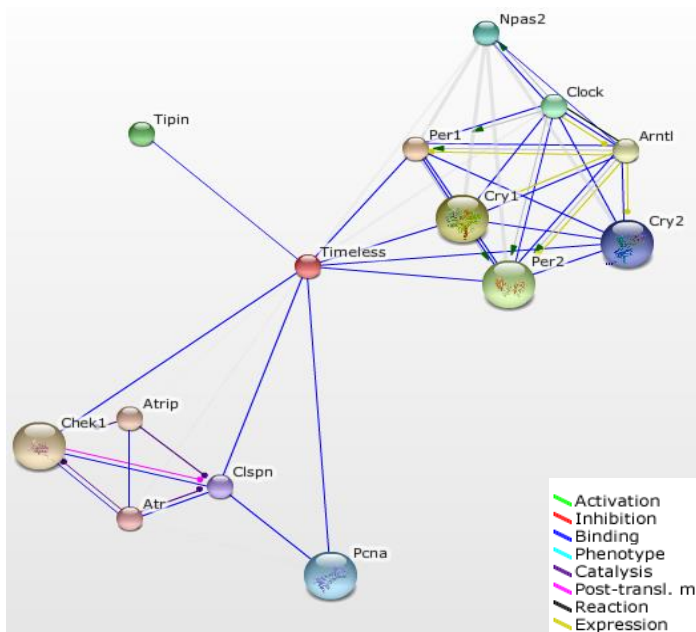
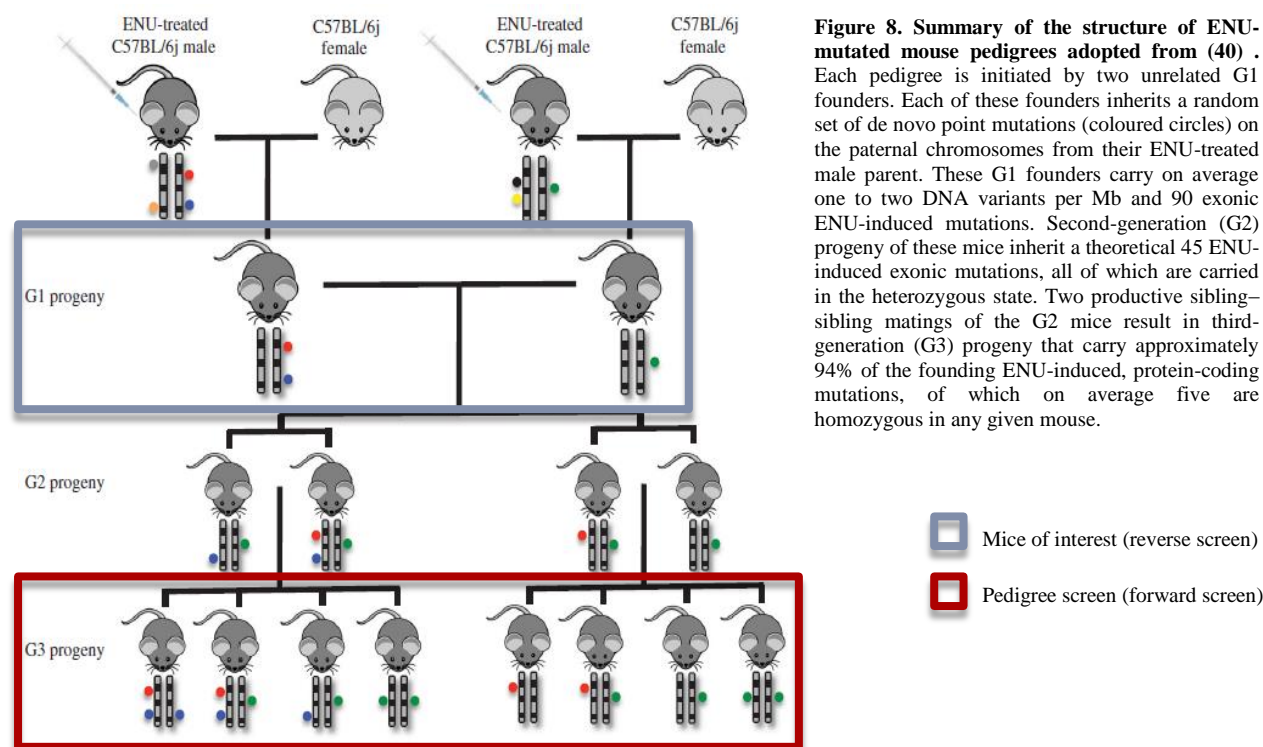


Figure 7. TIM protein interaction network. The network was developed using the String 9.05 database. The legend in the bottom right corner represents the type of interaction between different proteins.

### 3.2. ENU mutagenesis: going forward or reverse.

ENU mutagenesis in mice is used as a tool to find new genes (phenotype-driven/ 'forward genetic' approach) or validate the action of genes (gene-driven/ 'reverse genetic' approach) involved in specific pathology (37). This technique uses the alkylating agent N-ethyl-N-nitrosourea (ENU) that acts by transferring its ethyl group to any nucleophilic nitrogen or oxygen sites of nucleic acids (38). The transferred ethyl groups form random DNA adducts that can cause mispairing and, if not repaired, lead to mutations in spermatogonial stem cells during replication. The vast majority of ENU preferentially binds thymidine and produces one new mutation per gene (locus) per 200-700 gametes. Usually point mutations arise leading to missense/non-sense mutations or errors in splicing (38,39).



As such, the offspring can be screened for phenotypes of interest and the causative mutation can be investigated, i.e. a forward genetic screen for discovery purposes (Figure 7 red panel). The advantage of genome-wide screens using ENU mutagenesis is that it does not rely on prior knowledge or assumptions about the genes involved (37). This means that the likelihood of generating novel information is rather high.

ENU mutant mice are also suitable for validating if a gene has a role in specific disease. Performing ENU mutagenesis screens generates a sizable library of G1 founders with genome-wide aberrations (40) (Figure 8). Through NGS efforts, the presence of these gene aberrations in G1 mice have been verified and catalogued. The animals of interest (representing the mutant gene of interest) can be accessed by researchers for validation studies. This resource provides researchers with an extensive choice of gene aberrations, readily available for study.

### 3.3. Study aim and workflow

The aim of this master thesis is the discovery and validation of potential driver mutations/genes for a possible role in pancreatic tumourigenesis, using mice derived from ENU mutagenesis screens. The left panel of Figure 9 portrays the different steps and options for performing a discovery approach. ENU mutant mice are screened for a phenotype of early pancreatic tumourigenesis, i.e. ADM and/or hyperproliferation of the acinar portion of the pancreas. The right panel of Figure 9 pictures the use of ENU mutant mice for validation approaches. We have used this to validate if Timeless has a role in PDAC initiation, i.e. in ADM .

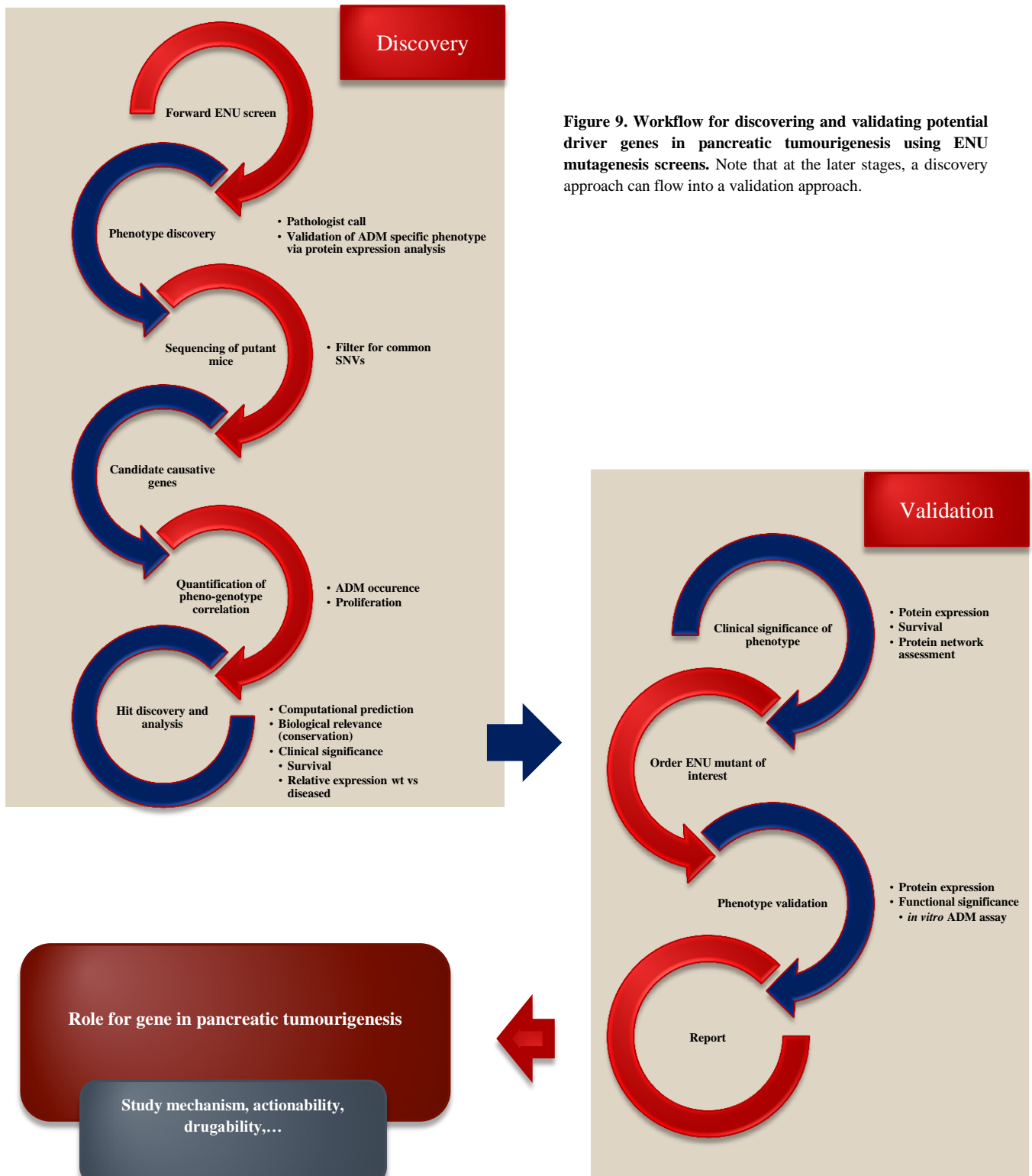


Figure 9. Workflow for discovering and validating potential driver genes in pancreatic tumourigenesis using ENU mutagenesis screens. Note that at the later stages, a discovery approach can flow into a validation approach.

## 4. Material and methods

### 4.1. ENU mutant mouse generation

ENU mutant mice were generated by treating pure C57BL/6j male mice with the mutagen N-Ethyl-N-nitrosourea (ENU) at the 'Australian Phenomics Facility' (APF) of the 'Australian National University' (ANU) as described in (40,41). Exome enrichment and sequencing, Single-nucleotide variant detection workflow and variant validation were performed by the APF of the ANU as described in (40,41).

### 4.2. Acinar cell isolation and culture

#### *4.2.1. Animals*

Pancreatic acinar cells were isolated from 8-12 week-old ENU mutant mice (APF). All experiments were performed in accordance with the institutional ethical committee and Australian national guidelines and regulations.

#### *4.2.2. ADM assay*

Acinar cell cultures were prepared as described previously (20). Whole pancreata were harvested and digested in 1,25 mg/ml collagenase-P (Roche, Castle Hill, NSW) for 20min at 37°C. After washing with 5% fetal bovine serum (FBS) (Gibco BRL, Gaithersburg, MD) supplemented Hanks balanced salt solution (HBSS), collagenase-digested pancreatic tissue was filtered respectively through 500 µm and 100 µm polypropylene mesh (Spectrum Laboratories, Laguna, CA). The filtrate was recovered after centrifugation on 30% FBS in HBSS at 1000 rpm for 2min. The cellular pellet constituted of viable acinar cells was resuspended in RPMI1640 glutamax medium supplemented with 1% pen/strep, 1% sodium pyruvate, 25µg/ml geneticin sulphate (all Gibco BRL, Gaithersburg, MD), 10% heat-inactivated fetal bovine serum (Sigma aldrich, Saint louis, MO). The cellular suspension was supplemented with 0.1 mg/ml soybean trypsin inhibitor (Sigma Chemicals, St Louis, MO) before starting culture. Suspension and monolayer cultures were maintained at 37°C and 5% CO<sub>2</sub> respectively for 5 and 7 days. RNA and protein lysate collections were performed on day 1 (before culture), 5 and 7. Media was changed on days 3 and 5.

### 4.3. Cell lines and inducible expression systems

#### *4.3.1. Overexpression construct*

*GUCD1* cDNA was amplified by PCR from total cDNA of HCT-116 human small intestinal cell line (ATCC® CCL-247™), using Phusion® high-fidelity DNA polymerase (Thermo Fisher Scientific, Inc, Waltham, MA). The following primers were used: forw: ATAGATATCGCCACCATGAGGACGGAGGCRGAGGCA; rev: TAGATATCTTAAGCATAATCTGGAACATCATATGGATAGCTGTCCARGTAGACAAAGAG

G. Insert amplification generated a 770 bp HA-tagged PCR product containing EcoRV restriction site on each end. The complete cDNA was cloned into the pENTR™-2b entry vector (Life Technologies, Rockville, MD) containing the kanamycin resistance gene. Subsequently *GUCD1-HA* was subcloned in the Rix-pTF-*EBR* lentiviral vector (42), containing a Blasticidin (BSD) resistance gene, using gateway cloning technology (Life Technologies, Rockville, MD). Corresponding amplicon concentration was verified with the Nanodrop2000 (Thermo Fisher Scientific, Inc, MA, USA). The vectors were transformed by heat shock in  $\alpha$ -select chemically competent cells (Bioline Inc., USA). The authenticity of the *GUCD1-HA* sequence was confirmed by sequencing.

#### 4.3.2. Knockdown construct

We used the pSlik system to generate the knockdown construct for mouse and human *GUCD1*. The vectors were designed to generate short hairpin RNA specific to the following target sequences of the *GUCD1* coding sequence: TGAGGACATCCTCTTTGTCTAC and CGAGGACATCCTCTTTGTCTAC (43).

#### 4.3.3. Virus Production

Lentiviruses were produced in HEK293T cells (ATCC® ACS-4500™) as described before (43). Briefly, HEK293T cells were transfected by calcium phosphate method using the PSPAX2 as packaging vector, pCAG-VSVG as envelope plasmid and Rix-pTF-*GUCD1-HA-EBR* as transfer vector. Media was changed 24h post transfection. The viral supernatant was collected at 48h, filtered through 0.45µm, and stored at -80°C or directly put on the cells.

#### 4.3.4. Transduction of 266-6 mouse pancreatic acinar cell line

Rix-pTF-*GUCD1-HA-EBR* lentivirus was directly added to 266-6 acinar cells (ATCC® CRL-2151™) in a 6-well plate. 266-6 is an acinar pancreatic cell line derived from a young adult mouse whereby the cells were immortalised with an elastase I/SV-40 T antigen fusion gene (44). The cells were incubated at 37 °C, 5% CO<sub>2</sub> for 72h. Blasticidine S Hydrchloride (BSD) (Sigma Chemicals, St Louis, MO) was used at 5µg/ml final concentration to select transduced cells. After 7 days, expression of HA-tagged *GUCD1* (*GUCD1-HA*) was induced by adding Doxycycline Hyclate (dox) (Sigma Chemicals, St Louis, MO) at 1µg/ml final concentration.

### 4.4. Immunostainings

#### 4.4.1. Immunohistochemistry (IHC)

Tissues were fixed in buffered 4% formaldehyde and processed for paraffin embedding. Depending on the primary antibody used, heat-induced epitope retrieval was performed using regular heat, waterbath or pressure cooker of paraffin sections in s1699 (pH6) or s2199 (pH9) buffer (DAKO, Glostrup, Denmark). All primary antibodies were visualized using the DAKO envision system (DAKO, Glostrup, Denmark) and 3,3'-diaminobenzidine (DAB) as substrate (DAKO, Glostrup, Denmark). Stainings were performed on the DAKO autostainer universal staining system (DAKO, Glostrup, Denmark) or Leica bond RX system (Leica, Wetzlar, Germany). Only Krt19 antibody was

visualized using goat-anti rat HRP antibody (Thermo Fisher Scientific, Inc, Waltham, MA). Images were acquired using the Scanscope FL (Aperio, Vista, CA). A list of antibodies used is shown in Table 2.

#### 4.4.2. Proliferation quantification

Ki67 positive cells were counted in 7 different random microscope fields of two sections (magnification 20x) for each mouse pancreas. Generated data was transported into GraphPad Prism for statistical analysis. The proliferation count is the cumulated number of ki67 positive cells in all counted fields per mouse.

#### 4.4.3. Immunofluorescence (IF)

$3 \times 10^4$  cells were plated in a 24-well plate and grown to sub-confluency. Cells were fixed in 4% buffered formaldehyde (Sigma Chemicals, St Louis, MO) at room temperature for 15 min. Afterwards cells were permeabilized with 0.5% TRITON X-100 (Sigma aldrich, Saint louis, MO) in PBS (Gibco BRL, Gaithersburg, MD). Depending on the primary antibody used, unspecific binding sites were blocked in 2% BSA (Sigma aldrich, Saint louis, MO) or 10% FBS (Gibco BRL, Gaithersburg, MD) in PBS. All primary antibodies were incubated for 1 hour at room temperature (RT) in a humid chamber. Specifically bound primary antibodies were subsequently detected by incubation with Cy3-labelled goat anti rat (Invitrogen, Life Technologies, Rockville, MD) at RT for 45 minutes. Nuclei were counterstained with 4,6-diamidino-2-phenylindole (DAPI) (Invitrogen, Life Technologies, Rockville, MD) in 1/500 dilution for 5 min. Coverslips were mounted using Prolong antifade gold (Invitrogen, Life Technologies, Rockville, MD). Images were obtained using a Leica DM5500 fluorescence microscope (Leica, Wetzlar, Germany).

### 4.5. Real-time reverse transcription polymerase chain reaction (RT-qPCR)

Total RNA was isolated using the Purelink™ RNA mini kit (Life Technologies, Rockville, MD) with DNase treatment following manufacturer's instructions. RNA concentration was assessed using Nanodrop2000 (Thermo Fisher Scientific, Inc, MA, USA). When whole pancreas was processed, total RNA isolation was performed using phenol/chloroform extraction followed by purification with the Purelink™ RNA mini kit. cDNA was prepared by random priming from 20 ng RNA-equivalent using the superscript III First-Strand cDNA Synthesis kit (Life Technologies, Rockville, MD) in 20 µl of reaction mixture containing dNTP (200 µM each). 10ng cDNA was used for qPCR with specific primers (Table 1) in the presence of SYBR GreenER (Life Technologies, Rockville, MD) using the 7900H Fast Real Time PCR System (Life Technologies, Rockville, MD). All analyses were done in duplicate. Melting curve analysis was performed for each reaction to control for product quality and specificity. The expression levels were normalized to the expression of the house keeping gene (Hprt).

Gene	Forward primer	Reverse primer
Hprt	GGC CAG ACT TTG TTG GAT TTG	TGC GCT CAT CTT AGG CTT TGT
Cpa1	TAC ACC CAC AAA ACG AAT CGC	GCC ACG GTA AGT TTC TGA GCA
Amy2	TGG CGT CAA ATC AGG AAC ATG	AAA GTG GCT GAC AAA GCC CAG
Krt7	CAC GAA CAA GGT GGA GTT GGA	TGT CTG AGA TCT GCG ACT GCA
Krt19	CCT CCC GCG ATT ACA ACC ACT	GGC GAG CAT TGT CAA TCT GT
Pdx1	AAA TCC ACC AAA GCT CAC GC	CGG TCA AGT TCA ACA TCA CTG C
Sox9	TCG GTG AAG AAC GGA CAA GC	TGA GAT TGC CCA GAG TGC TCG
Gucd1	GCG CCA CTT TGG TGT GAG AC	GCG CCA GGT GTA CTT GGA TGT
Rbpjl	ATG CCA AGG TGG CTG AGA AAT	CTT GGT CTT GCA TTG GCT TCA
Ela1	CGT GGT TGC AGG CTA TGA CAT	TTG TTA GCC AGG ATG GTT CCC

Table 1. RT-qPCR primer list.

#### 4.6. One-dimensional sodium dodecyl sulfate polyacrylamide gel electrophoresis (SDS-Page) and Western Blot

Proteins from mouse 266-6 acinar cells, pancreatic tissue and primary cultured cells were extracted in lysis buffer (50 mM Tris-HCl pH 8,0, 150 or 650 mM NaCl, 5 mM EDTA pH 8,0, 0,5% NP-40, 0,1% SDS) supplemented with protease and phosphatase inhibitors (Complete, EDTA-free protease inhibitor cocktail and phosSTOP, Roche Diagnostics, Meylan Cedex, FR) and clarified by centrifugation. Protein lysate concentration was determined by Pierce® BCA protein assay kit (Thermo Fisher Scientific, Inc, Waltham, MA). Protein lysates were reduced in sample buffer and heated to 70°C. Afterwards protein lysates were separated under denaturing conditions via SDS-Page in 3-(N-morpholino)propanesulfonic acid (MOPS) or 2-(N-morpholino)ethanesulfonic acid (MES) buffer on Novex nuPage 4-12% bis-tris gels (Life Technologies, Rockville, MD). Protein was transferred via electroblotting and blotted onto a polyvinylidene fluoride membrane. Membranes were blocked in 5% skim milk and probed with primary antibodies overnight. Membranes were incubated with HRP-conjugated secondary antibodies (Perkin-Elmer, Waltham, MA.). Proteins were visualized using electrochemiluminescence (Perkin-Elmer, Waltham, MA.) and autoradiography.

##### *4.6.1. Densitometric quantification.*

Protein bands of the anticipated molecular weight were quantified with ImageJ software (version 1.38x). Protein quantities were expressed as a proportion of  $\beta$ -actin.

## 4.7. Antibodies

antibody	clonality	species	manufacturer	Working dilution		
				IHC	WB	IF
anti-HA (clone 3F10)	monoclonal	rat	Roche, Castle Hill, NSW	x	1/1000	1/200
anti- $\beta$ -actin	monoclonal	mouse	Sigma aldrich, Saint louis, MO	x	1/2000	x
anti-Ki67	polyclonal	rabbit	BD PharmingenFranklin Lakes, NJ	1/1000	x	x
anti-cytokeratin 19 (TROMA III)	polyclonal	rat	Developmental Studies Hybridoma bank, Iowa, IO	1/15	1/250	x
anti-Gucd1	polyclonal	rabbit	novus biologicals, Littleton, CO	1/25	1/500	1/25
anti-Gucd1	polyclonal	rabbit	Thermo Fisher Scientific, Inc, Waltham, MA	1/25	1/2000	x
anti-Sox9	polyclonal	rabbit	Millipore, Billerica, MA	1/10000	1/2000	x
anti-Timeless	polyclonal	rabbit	Bethyl laboratories, Montgomery, TX	1/100	1/1000	x
anti-Ptf1a	polyclonal	rabbit	Millipore, Billerica, MA	x	1/1000	x

**Table 2. Antibody list for IHC, WB and IF.** x means that the antibody was not used for this purpose.

## 4.8. Protein structure prediction

The protein structure prediction was generated using the newly developed protein structure prediction software Aquaria (<http://aquaria.ws:8009/Q96NT3> available starting july 2013; details can be requested at [sean@odonoghuelab.org](mailto:sean@odonoghuelab.org)). Protein binding sites were generated using I-tasser (45,46).

## 4.9. Statistical analyses.

Data were analyzed by two tailed Student t-test. Statistical significance was accepted at a  $p < 0.05$  (GraphPad Prism). Results are shown as mean  $\pm$  SEM. The number of independent experiments is indicated in the text as “n”.

## 5. Results

### 5.1. Driver gene discovery approach

#### 5.1.1. Phenotype presentation and causative mutation determination

Acinar to ductal metaplasia and dysplastic ductal proliferation was upfront determined as the ‘affected’ phenotype. Two male G3 mice of the 19WT29a pedigree (random nomenclature) were identified by a pathologist to be ‘affected’. We confirmed these findings by IHC on pancreata from these mice and observed an increase in protein expression of ADM markers (Sox9, Krt19) as well as an increase in proliferation, as analysed by Ki67 staining, compared to wild-type mice (Figure 10a). Ki67 staining was highly increased in the affected region. The increased Ki67 staining in the rest of the affected pancreas vs. wild type was less pronounced. This was quantified and found highly significant (\*\*p=0,0036) (Figure 10b).

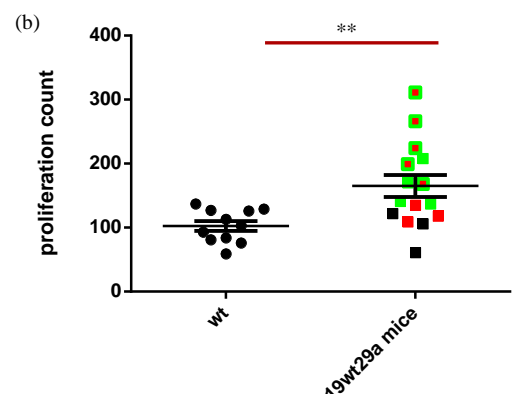
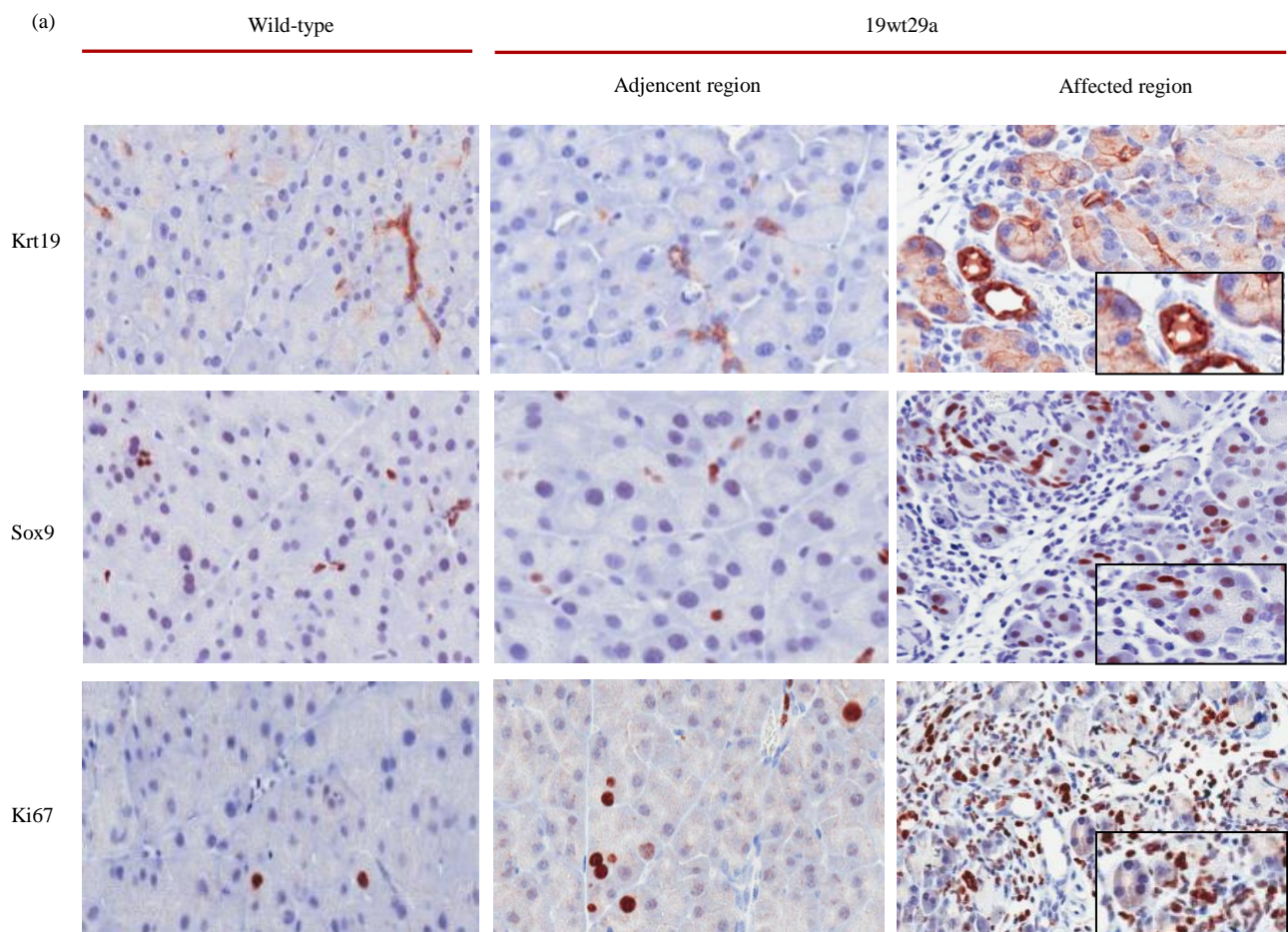


**Figure 10. Analysis of ADM and proliferation in affected 19wt29a mice.** Affected mice were assayed for the presence of ADM (Krt19, Sox9) and proliferation (Ki67) via IHC. Note that the affected region is localized. (b) Proliferating cells in the whole pancreas of the screened pedigree were quantified (\*\*p=0.0036). High proliferation is marked in green (cut-off value is highest value in wild types). Mice portraying ADM are marked in red. Mice positive for both are double coloured.

In order to determine the causative mutation, the two affected mice were sequenced at the APF. exome-wide distribution of SNVs was verified in both mice to exclude biased variant calling (see material and methods). Putative mutations for the phenotype were filtered for being homozygous in both mice or homozygous in one mouse and heterozygous in the other. Applying this methodology to our filtered list of variants we came up with two common homozygous mutations in both mice and three homozygous mutations in one but heterozygous in the other (Figure 11). The mouse gene *Zfp316* has no human homolog and was therefore discarded from further investigation. The other four candidate gene mutations have a known cell biology function or are uncharacterised (Figure 12).

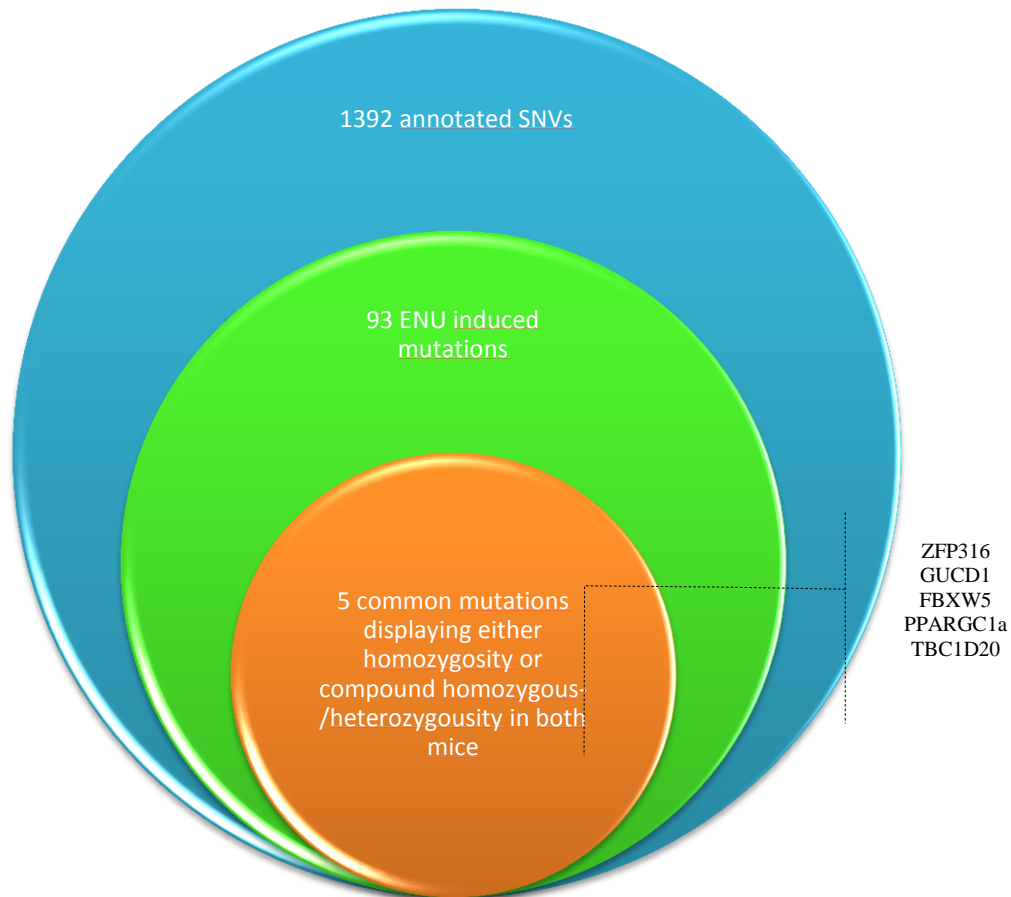


Figure 11. Summary outline of the SNV filtering strategy.

gene name	human homolog	mutation	amino acid change	gene description	gene ontology	validated genotype	
						mouse 1	mouse 2
Gucd1	GUCD1	C>G	R->P	Guanlyl cyclase domain 1	unknown	Hom	Hom
Tbc1d20	TBC1D20	T>C	N/A	TBC1 domain family, member 20 Gene	GTPase activator activity, Rab GTPase activator activity, integral to membrane, intracellular membrane regulation of Rab GTPase activity	Hom	Het
Ppargc1a	PPARGC1A	A>T	S->R	peroxisome proliferative activated receptor, gamma, coactivator 1 alpha Gene	DNA-dependent DNA binding, RNA binding, cellular response to oxidative stress, cytosol, ligand-dependent nuclear receptor binding, ligand-dependent nuclear receptor transcription coactivator activity, mitochondrion organization, negative regulation of neuron apoptosis, nucleic acid binding, nucleotide binding, nucleus, positive regulation of fatty acid oxidation, positive regulation of gene-specific transcription, positive regulation of gene-specific transcription from RNA polymerase II promoter, positive regulation of transcription, positive regulation of transcription factor activity, positive regulation of transcription from RNA polymerase II promoter, protein binding, respiratory electron transport chain, response to muscle activity, transcription activator activity, transcription coactivator activity	Het	Hom
Fbxw5	FBXW5	G>T	G->C	F-box and WD-40 domain protein 5 Gene	protein binding	Het	Hom

Figure 12. Candidate gene mutations and genotype validation.

We then narrowed our shortlist down by combining IHC proliferation data from a cohort of 15 ENU-treated mice in this putatively affected pedigree (19wt29a) (Figure 13). Our analysis showed that mutated *Gucd1* is the most likely candidate as causative gene. Animals harbouring this mutation were the only ones showing both ADM and high proliferation.

Homozygous and heterozygous	Total	<i>Gucd1</i>	<i>Fbxw5</i>	<i>Pparg1a</i>	<i>Tbc1d20</i>
ADM	8/15(53%)	7/8(88%)	4/8(50%)	4/8(50%)	4/8(50%)
high proliferation	9/15(60%)	8/9(89%)	7/9(78%)	3/9(33%)	4/9(44%)
ADM+proliferation	5/15(33%)	5/5(100%)	3/5(60%)	2/5(40%)	2/5(40%)
<b>Homozygous</b>					
ADM	8/15(53%)	5/8(62%)	1/8(12%)	2/8(25%)	1/8(25%)
high proliferation	9/15(60%)	4/9(44%)	2/9(22%)	2/9(22%)	2/9(22%)
ADM+proliferation	5/15(33%)	4/5(80%)	1/5(20%)	1/5(20%)	0/5(0%)
<b>Heterozygous</b>					
ADM	8/15 (53%)	2/8 (25%)	3/8 (38%)	2/8 (25%)	3/8 (38%)
high proliferation	9/15 (60%)	4/9 (44%)	5/9 (67%)	4/9 (44%)	2/9 (22%)
ADM+proliferation	5/15 (33%)	1/5 (20%)	2/5 (20%)	1/5 (20%)	2/5 (40%)

**Figure 13. Occurrence of candidate mutations in the analysed 19wt29a mouse population.** Mice were assayed for proliferation and the occurrence of a histological phenotype (ADM, high proliferation or both). Ratio in ‘Total’ column is the ratio of the number of mice presented with row specific phenotype vs all mice assayed in the affected pedigree (n=15). Ratio’s in the gene specific columns are the ratios of the number of mice harbouring the respective column mutation vs the number of mice having the row specific phenotype, i.e. of 5 mice having the *Gucd1* mutation, 5 presented with ADM and high proliferation (100%).

ENU-mice harbouring a mutation in *Gucd1* seem to exhibit high proliferation in the pancreas (Figure 14). As previously shown 19wt29a mice have higher proliferation compared to their wild-type littermates (not treated with ENU) (\*\*p=0.0036) (Figure 14a). Heterozygous *Gucd1* mutant ENU-mice did not show an increase in proliferation (p=0.1341) vs. wild-type whereas homozygous *Gucd1* mutant ENU-mice show a significant increase in proliferation (\*p=0.0121). The high proliferation in the homozygous *Gucd1* mutant population is also accompanied with the occurrence of ADM (Figure 14b). This data indicates that a homozygous *Gucd1* is the probable causative mutation for the perturbing phenotype.

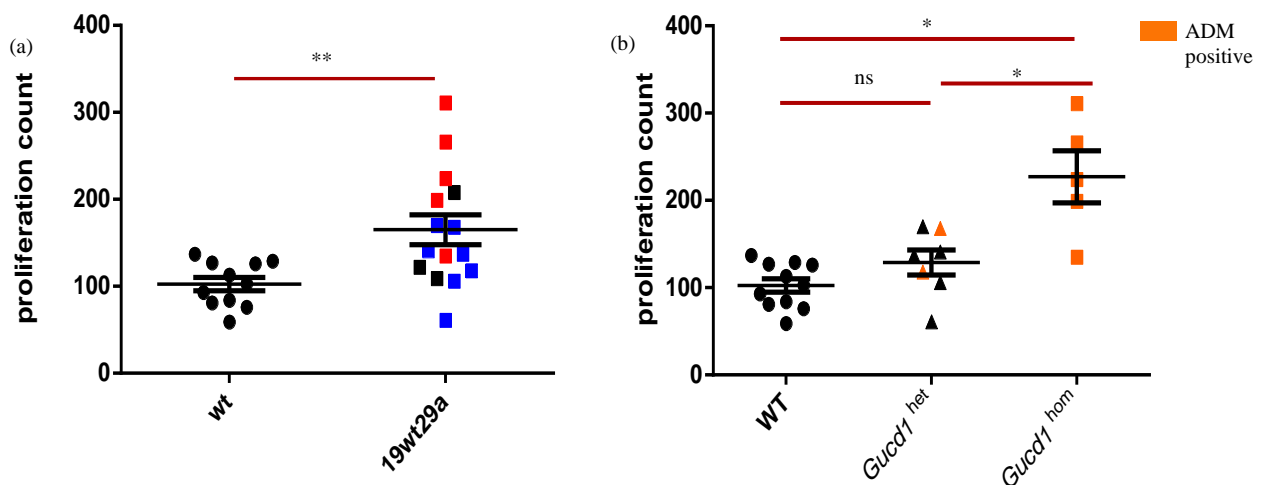


**Figure 14. Wild-type and 19wt29a mice were assayed for proliferation in the pancreas.** (a) Mice heterozygous for *Gucd1* were colored in blue. Mice homozygous for *Gucd1* are colored in red. (b) Heterozygous and homozygous *Gucd1* 19wt29a mice were compared vs. wild-types. Note: homozygous *Gucd1* 19wt29a mice vs. heterozygous \*p=0,0258.

5.1.2. Hit discovery and analysis

After our phenotype-genotype correlation, we went deeper into investigating our putative gene/mutation. *GUCD1* is an uncharacterised gene with a highly conserved functionally annotated domain (click [link](#)<sup>1</sup> for in-depth view). The mutation in the affected mice is a cytosine to guanine (C>G) transversion, which leads to an arginine (R) to proline (P) amino acid change at position 179 in the protein. This structural change implies the loss of a positive charge in the protein and an increase of the polarity in that region (Figure 15b). Figure 15a. shows the location of the R179P (red arrow) change in relation to the structural conformation of the predicted protein structure.

(a)

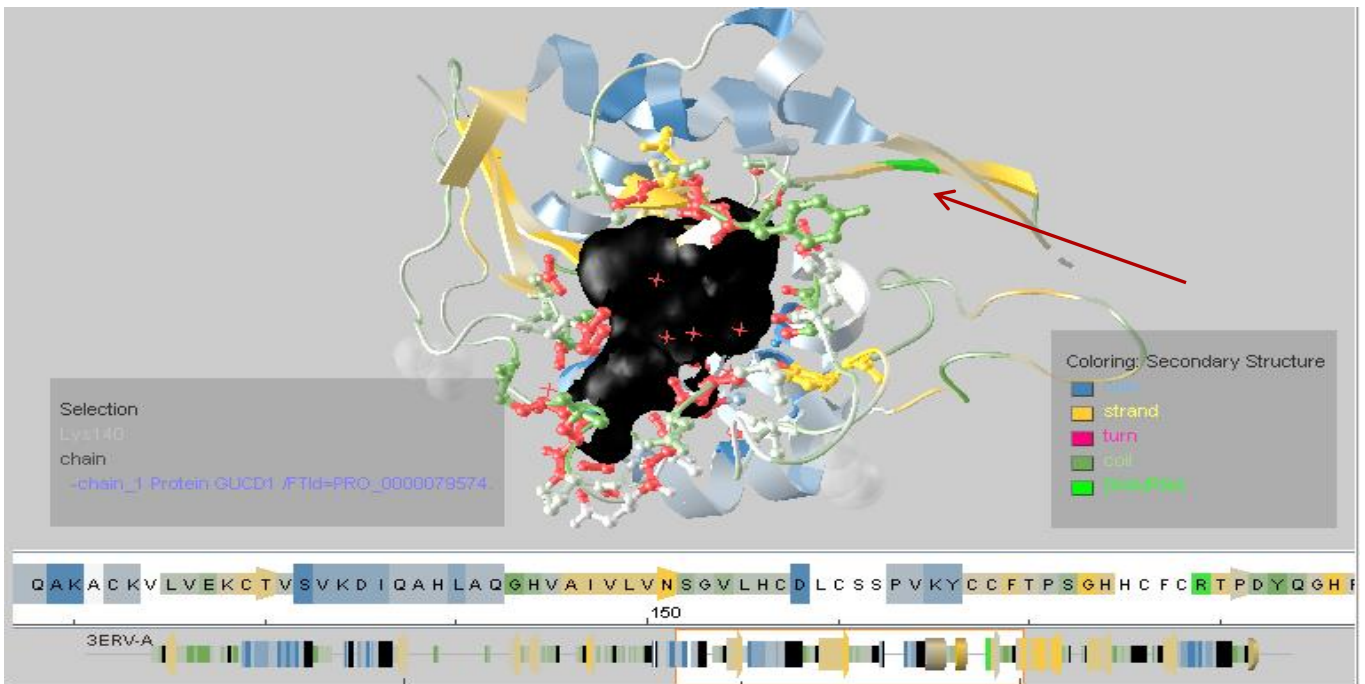
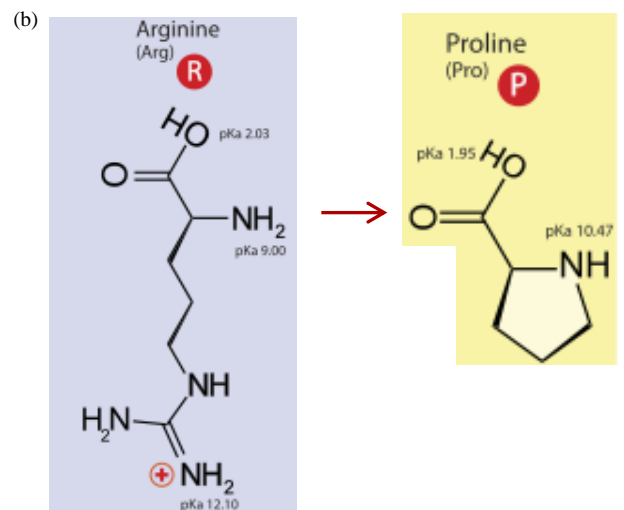


**Figure 15. Protein structure prediction for mouse Gucd1.** (a) By assessing the proximity of R179P in the wild-type protein relative to the predicted binding pocket, one could predict that a transition to P can have great impact on the protein structure. Residues marked in red define the 4Å proximity signifying the potential importance of those residues for normal protein function. (b) R>P transition can have serious structural consequences as demonstrated by their individual structural differences (<http://en.academic.ru/dic.nsf/enwiki/241090>).



<sup>1</sup> [http://asia.ensembl.org/Homo\\_sapiens/Gene/Comparative\\_Tree?db=core;g=ENSG00000138867;r=22:24936406-24951903](http://asia.ensembl.org/Homo_sapiens/Gene/Comparative_Tree?db=core;g=ENSG00000138867;r=22:24936406-24951903)

Although uncharacterised, *GUCD1* has been analysed in expression arrays and whole genome sequencing in diverse cancer studies. ‘The Cancer Genome Atlas’ mRNA expression data shows that *GUCD1* is altered in different types of cancer (47). In general, a plethora of cancers show amplifications of the gene. Mutations and deletions also occur. None of these alterations, however, are present at high frequency (Figure 16).

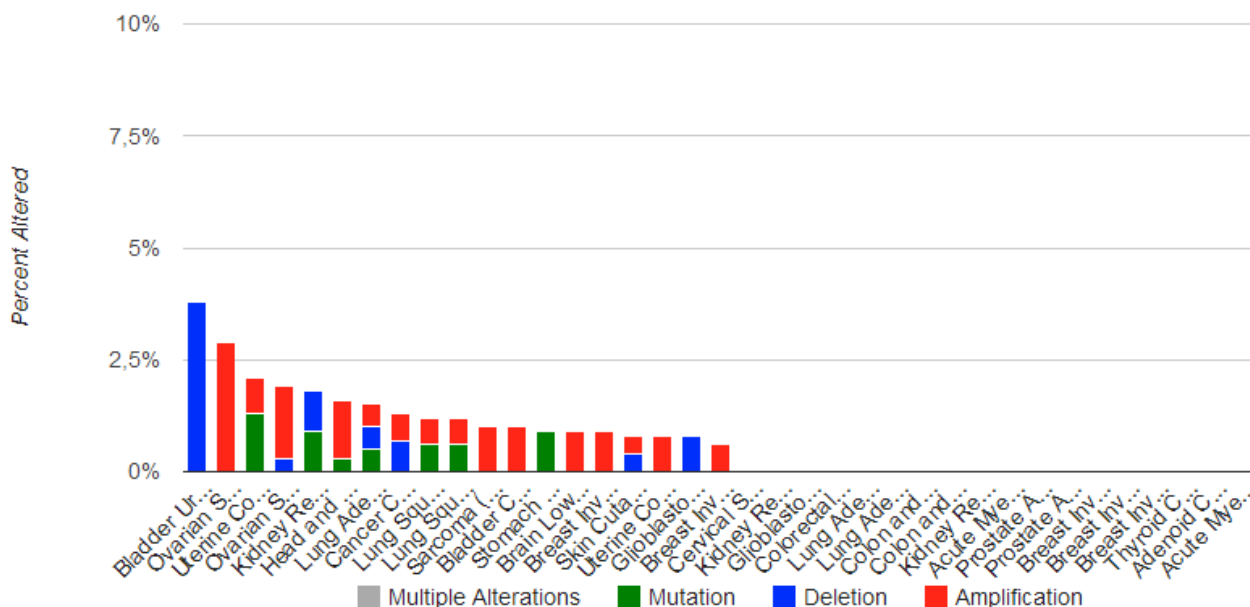


Figure 16. Percent of samples showing altered (mutation, deletion, amplification or multiple alterations) *GUCD1* mRNA expression for each cancer study with mutation data (48).

### 5.1.3. *GUCD1* mRNA expression analysis

In our ICGC cohort of 98 PDAC patients, we did not detect a *GUCD1* mutation. CNV is under analysis. We found in microarray analysis that *GUCD1* mRNA is highly expressed in the tumour as well as the adjacent tissue (data not shown). Kaplan-Meier survival curves were generated based on these mRNA expression data, using a 50% cut-off (Figure 17). This showed a tendency for better survival in patients with low *GUCD1* expression, although this was not significant ( $p=0.05775$ ).

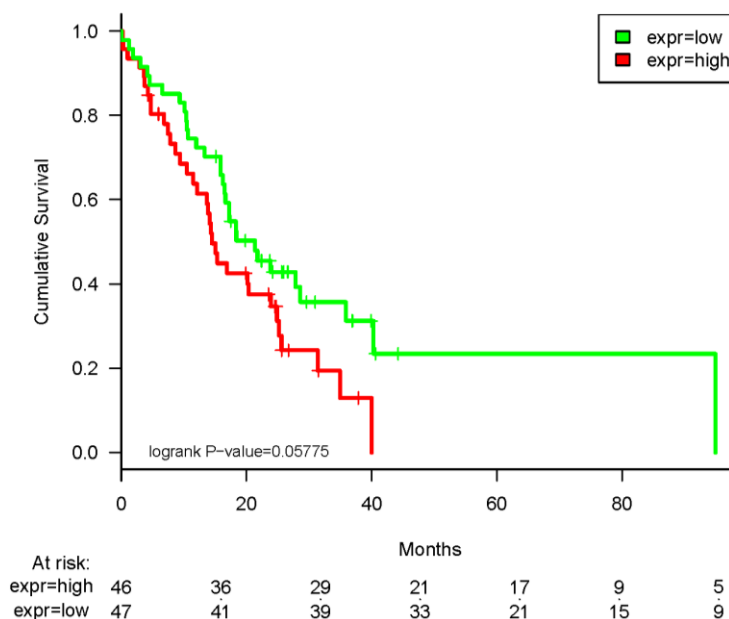


Figure 17. Kaplan-Meier curves showing overall survival of PDAC patients using mRNA expression of tumour resections at 50% cut-off.

We also assayed the mRNA expression of *Gucd1* in mouse models of ADM and pancreatic cancer by RT-qPCR (Figure 18). *Gucd1* shows decreased expression levels in these models compared to normal tissue. In the culture model, *Gucd1* expression decreases in suspension culture (\*\* $p < 0,0001$ ). Pancreata of animals where pancreatitis was induced by caerulein treatment showed decreased *Gucd1* mRNA expression (\*\* $p = 0,0001$ ) compared to normal pancreas. Similarly, pancreatic tumours from the KPC model also show decreased *Gucd1* mRNA expression (\*\* $p = 0,0004$ ) vs. normal pancreas. *Gucd1* mRNA level was significantly lower in pancreatic tumours compared to pancreata of caerulein treated mice (\* $p = 0,0154$ ).

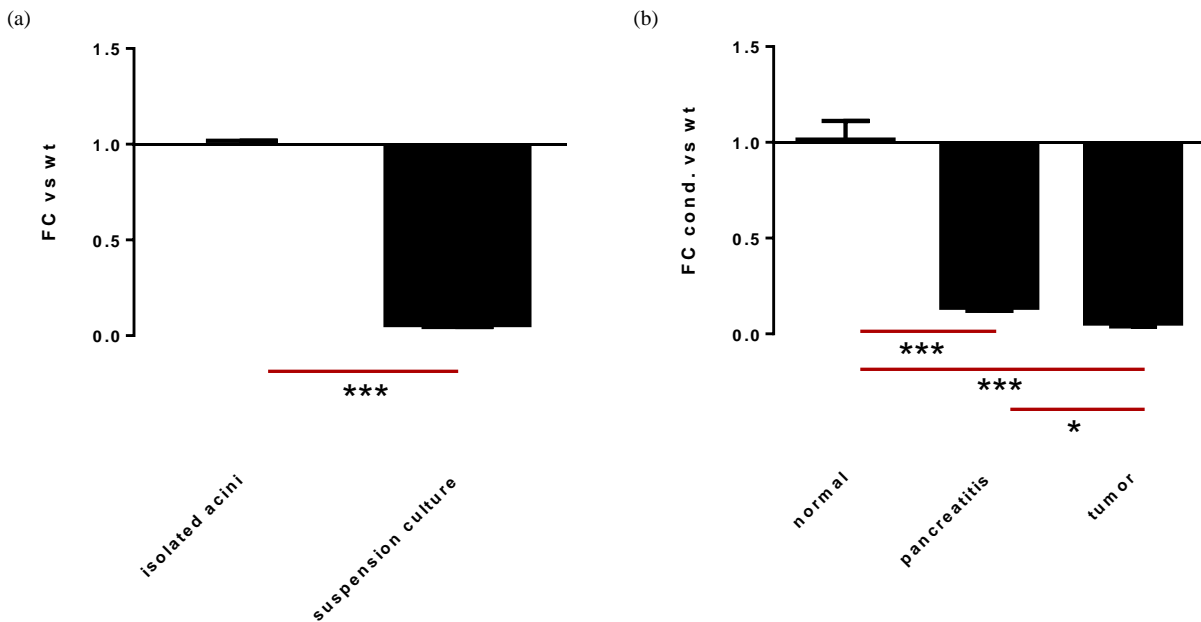
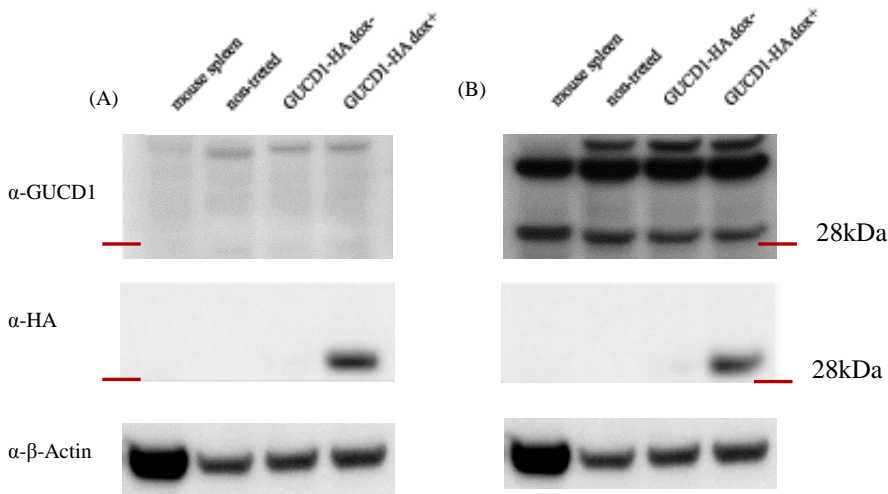


Figure 18. *Gucd1* expression is decreased in (a) a mouse culture model of ADM and (b) mouse models of pancreatitis and pancreatic cancer.

#### 5.1.4. Overexpression assessment of *GUCD1-HA* transduced 266-6 mouse pancreatic acinar cell line.

To gain further functional insights, we manipulated *GUCD1* expression in the 266-6 pancreatic acinar cell line. Knockdown experiments with shRNA failed. Transduction of the 266-6 acinar cells with a doxycycline (dox) inducible *GUCD1-HA* overexpression construct were successful. We assessed the extent of HA-tagged *GUCD1* by Western Blot. Using a HA-antibody we detected a band around 28kDa for the dox-induced construct. Commercial *GUCD1*-antibody A failed to show the expected band at the predicted molecular weight of 27kDa. Commercial *GUCD1*-antibody B picked up a band around the predicted molecular weight as well as many other (more intense) bands. The band around 27 kDa did not show increased intensity in the *GUCD1-HA* induced vs. the uninduced condition (Figure 19). Non-treated and *GUCD1-HA* uninduced conditions were negative in WB for the presence of the HA-tag, although RT-qPCR for *GUCD1* mRNA detected a low level of leakage in the uninduced condition (data not shown).



**Figure 19. GUCD1-HA protein expression after 1 week of dox treatment.** 266-6 acinar cells robustly express the transgene. Two different commercial antibodies (A and B) fail to detect GUCD1, whereas anti-HA only is detected in the GUCD1-HA+ dox condition. Mouse spleen cells were used as a positive control for antibody B corresponding to the manufacturers control. Samples were loaded on the same gel. Anti- $\beta$ -actin loading control was detected around 45kDa.

266-6 cells show green fluorescent staining for HA-tagged GUCD1 which is localised to the cytoplasm as indicated by the red arrow points. The variability in staining is probably due to the cells having various copy numbers of the viral construct. The green channel was overlaid with the DAPI channel visualizing the nuclei.

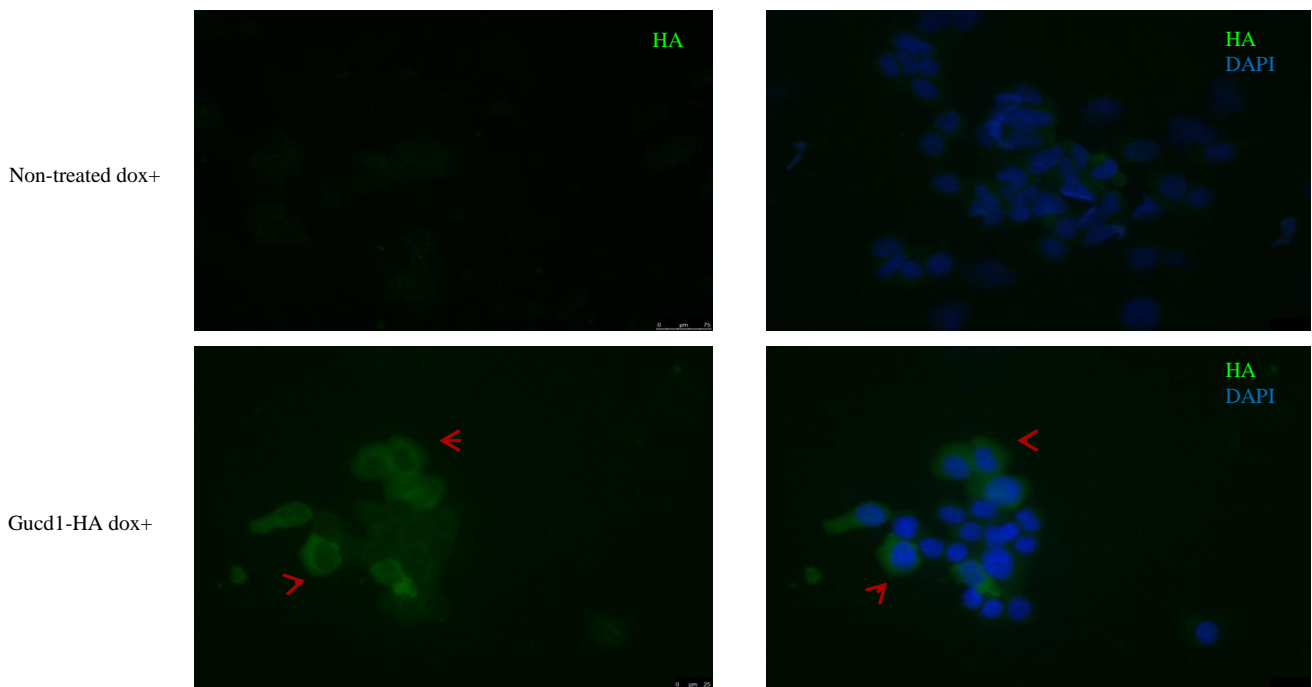


**Figure 20. Immunofluorescence for GUCD1-HA in 266 cells transduced with the inducible construct and in the non-treated dox+ condition.** Red arrow points indicate the high expressing GUCD1-HA protein cells. Scale shown in bottom right corner of green channel.

We predict that if GUCD1 would play a role in early pancreatic tumourigenesis, we might expect changes in acinar cell gene expression when overexpressing GUCD1. After 1 week of dox treatment, we did not detect differences (not shown). We then decided to re-assess mRNA and protein expression after 3 weeks of dox treatment (Figure 21). After 3 weeks of continuous induction GUCD1-HA is still significantly overexpressed (Figure 21a). RT-qPCR data show a distinct nonspecific dox effect on *Ptf1a*, *Sox9* and *Krt7* mRNA expression. Whereas we can observe a tendency of GUCD1-HA overexpression to downregulate the acinar enzyme *Cpa1* and the ductal specific *Krt19*, no consistent effect on the acinar phenotype is found.

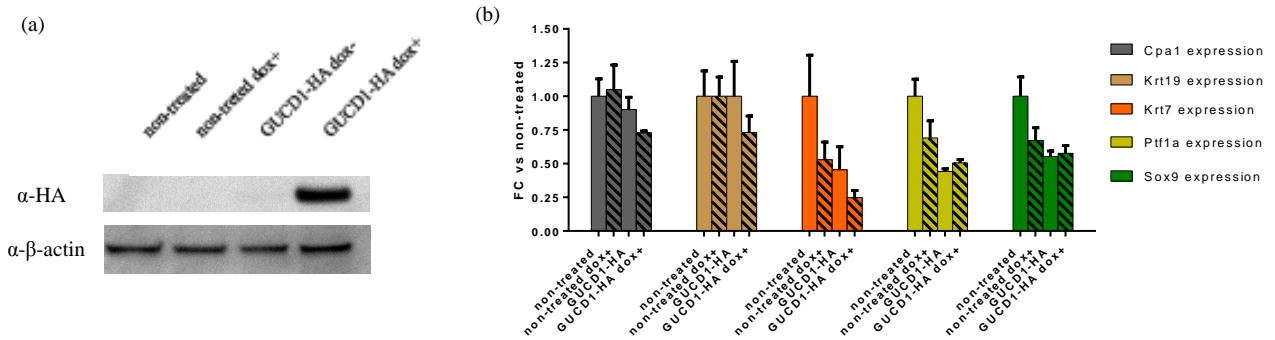


Figure 21. Protein (a) and mRNA (b) expression analysis of transduced 266-6 *Gucd1*-HA cells after 3 weeks dox treatment.

### 5.1.5. ADM assay of homozygous *Gucd1* mutant mice

As an alternative approach to assess the role of *Gucd1*, we obtained the homozygous *Gucd1* mutant mice and evaluated the effect of *Gucd1* mutation in the ADM assay using isolated pancreatic acinar cells of these animals and their controls. After 7 days of culture, we analysed mRNA expression levels of genes involved in ADM using RT-qPCR. *Gucd1* mRNA level was higher in the mutants (n=3) than in the wild-types (n=3) (\*\*p=0,0051). The acinar transcription factor *Ptf1a* as well as the enzyme *Amy2*, both known to be downregulated during ADM, were significantly more downregulated in day 7 cultures (\*p=0,0217 and \*p=0,0137, respectively). *Sox9* mRNA, known to be upregulated during ADM, was highly significantly more increased (\*\*p=0,0007). Together these data suggest that the mutant *Gucd1* acinar cells express more *Gucd1* and have more pronounced ADM features under stress.

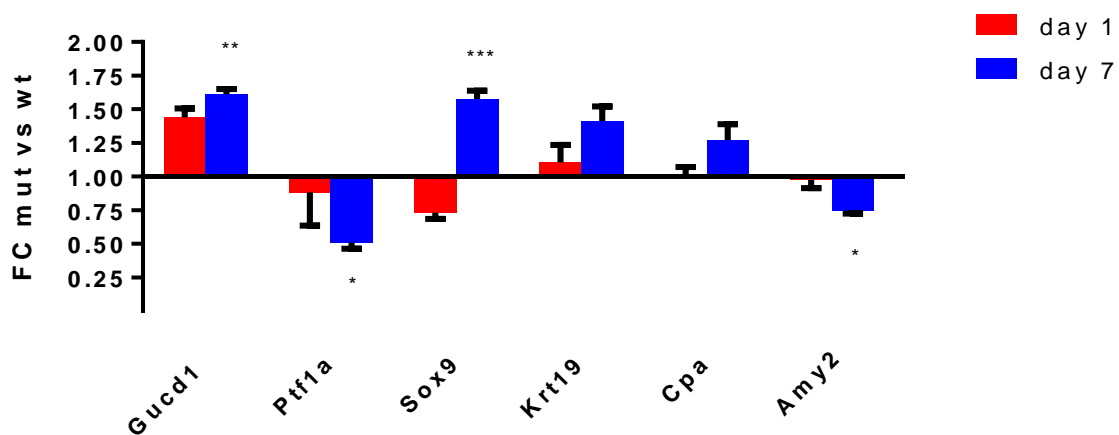


Figure 22. mRNA expression of a set of markers for ADM (*Sox9*, *Krt19*), pancreatic progenitor (*Ptf1a*) and acinar enzymes (*Cpa1*, *Amy2*) in mutant *Gucd1* mice compared to wild-type. Each bar represents the ratio between mutant and wt expression level per gene

## 5.2. Validation approach of Timeless as potential driver gene in pancreatic tumourigenesis using ENU mutagenesis.

### 5.2.1. Timeless protein expression in the pancreas of heterozygous *Tim* mutant mice

*Tim* mutant mice, obtained through ENU mutagenesis, presented with a heterozygous missense (T>C) mutation. The mutation was determined to be ‘probably damaging’ by computational prediction methods (48). The leucine to proline (L>P) amino acid change at position 219 causes the protein to lose a positive charge which could have consequences for normal protein function. All but one homozygous mouse died before birth. Histological assessment of the pancreas of heterozygous mutants did not reveal apparent differences.

Assessment of Timeless protein expression by IHC showed a strong nuclear *Tim* protein expression in the wild type mice. *Tim* heterozygous mutants seemed to exhibit decreased nuclear staining in the pancreatic tissue. This observation was also assessed by WB (Figure 23b). Densitometry of the blot showed *Tim* expression, to be slightly lower in *Tim* mutants vs. wild-type although this was not significant.

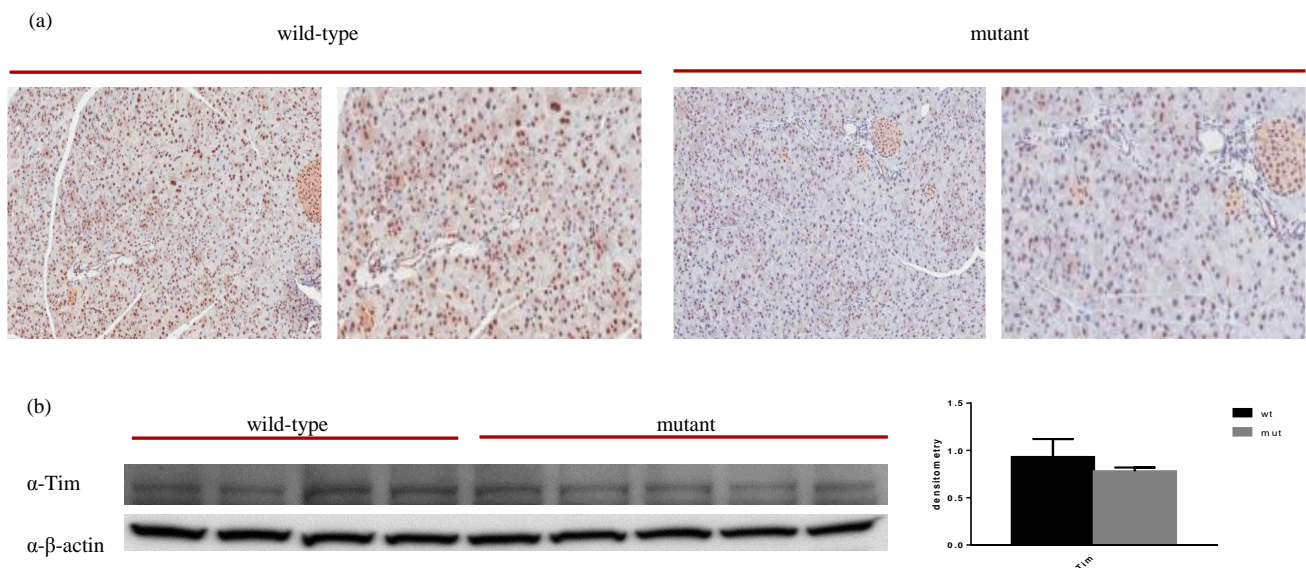


**Figure 23. Whole pancreas *Tim* protein expression.** (a) Strong expression of *Tim* in wild-type mice (left picture 20x and right picture 40x magnified for each condition). Staining appeared to be less intense in the mutant. (b) This was tested via Western Blot though did not reach significance in densitometry results (n=4-5).

### 5.2.2. *In vitro* ADM assay and whole pancreas analysis

In order to functionally validate the role of *Tim* in pancreatic tumourigenesis, we assayed heterozygous *Tim* mutant mice (n=3) together with their wild-type littermates (n=3) in our *in vitro* ADM assay (day 1 and day 7 of culture). We note that homozygous *Tim* mutants are lethal, therefore, we had to use heterozygous *Tim* mutant mice. In addition to the cultures, we compared whole pancreas tissue from heterozygous *Tim* mutant mice (n=5) with wild-type littermates (n=4) (red bars, Figure 24). Samples harvested on different time points were analysed for mRNA expression using RT-qPCR (Figure 24).

Sox9 mRNA expression is significantly increased in the whole pancreas (wp) of the mutant mice ( $*p=0.0318$ ), as well as increased in cultured cells ( $**p=0,0035$ ) of mutant versus controls (Figure 24a). Cells in culture also exhibited significant increases in another ductal marker, Krt19 ( $*p=0,0454$ ). Whereas not different in whole pancreas, analysis of freshly isolated acini (d1 of culture) showed a significant decrease in Ptf1a ( $**p=0,0098$ ) mRNA in the Tim mutant mice vs. wild-type (Figure 24b). This difference does not persist during culture. All other analysis did not show any significant differences.

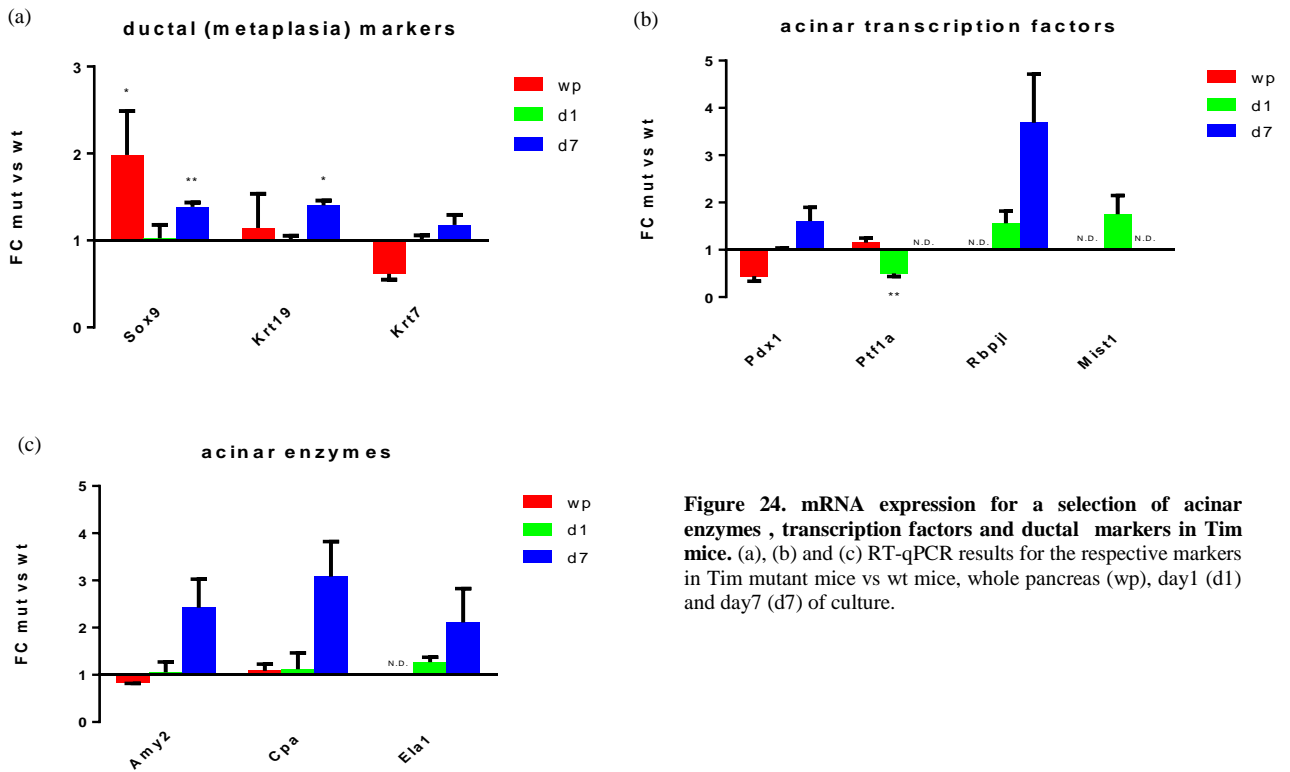


**Figure 24.** mRNA expression for a selection of acinar enzymes , transcription factors and ductal markers in Tim mice. (a), (b) and (c) RT-qPCR results for the respective markers in Tim mutant mice vs wt mice, whole pancreas (wp), day1 (d1) and day7 (d7) of culture.

## 6. Discussion

Although the endeavour continues to cure PDAC at any disease stage, succeeding in this goal still lies far in the future. The great challenge for managing pancreatic cancer in the absence of curative therapy is to be able to understand development of the tumour and detect precursor lesions before the advancement to metastatic disease. PDAC is characterised by an extensive genomic heterogeneity among different patients. The diversity of genomic aberrations among human PDAC samples, as described by Jones et al. and Biankin et al., precludes the identification of novel high frequent causative mutations (30,49). Nevertheless, identification of new important drivers/pathways, albeit only present in a subset of tumours, will aid the understanding of the tumour biology.

ENU mutagenesis is a powerful tool for generating random genomic mutations in mice (37,40). We used this tool to screen for phenotypes of interest such as ADM and hyperproliferation/dysplasia of ducts in the exocrine pancreas of ENU mutant animals. Because of the critical role of altered acinar cell differentiation and proliferation in PDAC initiation, this approach could allow us to pinpoint novel genes important in PDAC development (discovery approach). Alternatively, we also used ENU mutants (validation approach) to study genes of interest (here, Timeless) that came up in the genome sequencing analysis of PDAC patient samples.

In our discovery approach, as part of a collaborative study, we identified an ‘affected’ pedigree, i.e. showing focal ADM and hyperproliferation. A shortlist of candidate causative mutations in this pedigree was identified before commencement of this thesis. We then further investigated the common homozygous/heterozygous mutations in a larger panel of mice in this pedigree to relate phenotype to genotype. One of the possible causative mutations in *Zfp316* was excluded because this gene did not have a human homolog. It could have been a more cautionary action to actually include all genes in the analysis. Nevertheless, a homozygous mutation in the uncharacterised gene *Gucd1* presented features of being the common causative hit. *Gucd1* was significantly correlated with the ‘affected’ phenotype. We confirmed that the presence of ADM and high proliferation in the exocrine pancreas, by immunohistochemistry (IHC) for specific markers, specifically correlated with mutations in the *Gucd1* gene. *Gucd1* has only recently been named after its protein structure that corresponds to a domain encoding for a guanylyl cyclase (GUCD1= Guanylyl cyclase containing domain 1). No studies report on *Gucd1*, so it is unclear whether *Gucd1* has any functionality as a true guanylyl cyclase. Several studies have examined established members of the guanylyl cyclase family in pancreas (50) and as possible therapeutic targets in colon cancer (51).

At the outset of this thesis, the publicly available data for the thus far uncharacterised gene *GUCD1* (before *c22orf13*) was limited to expression arrays that indicated high gene expression in the intestine and the pancreas. Our RT-qPCR data on mouse pancreatic tissue/cells also suggested high mRNA expression with Ct values comparable to those of the housekeeping genes (e.g. *Hprt*). Unfortunately, we were unable to verify expression at the protein level due to questionable commercially available antibodies raised to GUCD1 that failed to detect a specific band in Western Blot analysis. When tested in IHC, one of the antibodies did reveal cytoplasmic staining of human small intestinal enterocytes, however pancreatic tissue was negative (data not shown). Analysis of GUCD1 was therefore limited to targeted RT-qPCR and microarray analysis.

In the microarray data available in our group, we observed that the expression of GUCD1 mRNA is high in PDAC and the high expressers have a tendency for lower survival outcomes. Our further analysis showed that ENU mutant mice express more *Gucd1* than their controls when subjected to

the ADM assay and display a more pronounced ductal phenotype in this assay. The latter is in agreement with the initial observations in the ENU screen. Specifically, results of the ADM assay showed *Gucd1* had an increased expression in the mutant cultures accompanied with the elevation of the ductal fate marker *Sox9* and a decrease of the acinar transcription factor *Ptf1a* and the acinar enzyme *Amy2*. These changes hint the enhanced progression to a 'ductal'-like phenotype. Recent studies unveiled a role for *Sox9* in maintaining ductal morphology and regulating duct-specific genes, suggesting that this transcription factor might have a similar function during acinar cell conversion into PanINs (52–54). As *Sox9* induces the expression of *Krt19* one would expect the latter to be increased in this assay. Indeed we can appreciate an increase in *Krt19* levels although not significant ( $p=0,068$ ). We can speculate that using more animals and harvesting at a later time point could have produced this significant result.

Based on these results one would conclude that mutant/higher *Gucd1* predisposes to develop conditions associated with pancreatic cancer initiation (ADM and high exocrine cell proliferation). This agrees with a lower outcome for high *GUCD1* expressing tumours. This seems however in contrast to the observations in Figure 18 where *Gucd1* expression decreases in ADM and tumour development in our established mouse models. Further functional assessment, including knockdown experiments are warranted to clarify this.

Where our attempts for knockdown failed, we succeeded in overexpressing *GUCD1* in the acinar cell line but this did not show any conclusive results. Using Western Blot, we identified an HA-band around the predicted molecular weight of 27kDA only present in the induced condition. Given the 96% similarity of amino acid alignment when comparing human and mouse *GUCD1*, we assumed that the human *GUCD1* overexpression in the mouse cell line should not be of any concern. We did not observe consistent significant changes in acinar cell phenotype with one acinar differentiation marker being suppressed, but also a ductal marker being suppressed. Given that our preliminary data show that the mutant *Gucd1* mouse pancreatic cells have higher *Gucd1* expression and increased exocrine cell proliferation, the overexpressing *GUCD1* cell line needs to be examined in the future for possible effects on proliferation.

We also tried to get more insights in the protein structure and localisation of *Gucd1* by protein structure prediction software and found that our mutation of interest is located near the predicted functional binding site of the protein. This may provide valuable information once the biochemical actions of this protein are further unravelled.

In conclusion, we identified a new gene that may be involved in PDAC development. Mutant *Gucd1* mice seem to develop ADM and have higher proliferation in the exocrine pancreas. The *Gucd1* mutants seem to have higher expression of *Gucd1* (at least when examined in the ADM assay). Higher expression is also related to worse patient outcome. These characteristics suggest an oncogenic effect. Further research is needed to assure its role, especially since this gene already seems to be highly expressed in normal pancreas tissue and expression was found downregulated in commonly used models, somewhat contradictory observations.

In the second part of this thesis, we undertook a validation approach where we studied the circadian gene *TIMELESS* in ENU-induced *TIM*-mutants. There was some preliminary evidence that *TIM* may be important in pancreatic cancer. The gene was affected by mutation/CNV in about 10% of patient tumours. Moreover, there was strong inverse correlation between protein expression and survival. We note that caution is needed when examining expression of proteins that are influenced by the circadian rhythm. Despite this, the fact that *TIM* may be drugable through the use of *CHK1*

inhibitors sparked further interest. Recent approaches in personalised medicine aim to detect patient tumour specific mutations that are drugable, rather than treating all PDACs with one drug.

We used an ENU-induced mutant in the *TIM* gene to embark on the study of TIM in pancreatic cancer. The ENU mutant was confirmed by prediction models to be functionally compromised. Death of all but one homozygous mutant strengthens this assumption.

Whereas our preliminary analysis in the mouse mutant shows loss of Tim expression, the patient in our cohort that presented with the *TIM* mutation displayed high protein expression. This underscores the fact that inclusion of the ENU mutants nowhere aims at representing the patient specific mutation. It is merely used as a model for ‘altered’ expression of a given gene of interest.

As a first assessment, we evaluated acinar and duct cell specific gene expression in the *Tim* mutant versus wild type pancreas. Similar analysis was performed on acinar cells undergoing the *in vitro* ADM assay. Higher *Sox9* mRNA expression seemed to be consistent in these samples. Further validation of this observation at the protein level needs to be performed. However, there is little other evidence to pursue this gene’s role in ADM or tumour initiation. The clinical data for TIM still makes it a potential target for investigation in association with tumour progression and a role in established tumours.

In conclusion, ENU mutagenesis was used as a tool for the discovery and the validation of candidate genes for their involvement in pancreatic tumourigenesis. Both approaches showed potential. The study of *Gucd1* as a novel not yet characterised gene is worth to be continued.

## 7. References

1. Jemal A. Global Cancer Statistics (vol 61, pg 69, 2011). *Ca- Cancer J Clin*. 2011 Mar;61:134–134.
2. Michl P, Gress TM. Current concepts and novel targets in advanced pancreatic cancer. *Gut*. 2013 Feb;62:317–26.
3. Lowenfels AB, Maisonneuve P. Epidemiology and risk factors for pancreatic cancer. *Best Pr Res Clin Gastroenterol*. 2006 Apr;20:197–209.
4. Michaud DS, Liu SM, Giovannucci E, Willett WC, Colditz GA, Fuchs CS. Dietary sugar, glycemic load, and pancreatic cancer risk in a prospective study. *J Natl Cancer I*. 2002 Sep 4;94:1293–300.
5. Michaud DS, Giovannucci E, Willett WC, Colditz GA, Stampfer MJ, Fuchs CS. Physical activity, obesity, height, and the risk of pancreatic cancer. *JAMA*. 2001 Aug 22;286:921–9.
6. Burris HA, Moore MJ, Andersen J, Green MR, Rothenberg ML, Modiano MR, et al. Improvements in survival and clinical benefit with gemcitabine as first-line therapy for patients with advanced pancreas cancer: a randomized trial. *J Clin Oncol*. 1997 Jun;15:2403–13.
7. Hezel AF, Kimmelman AC, Stanger BZ, Bardeesy N, Depinho RA. Genetics and biology of pancreatic ductal adenocarcinoma. *Genes Dev*. 2006 May 15;20:1218–49.
8. Morris JP, Cano DA, Selkine S, Wang SC, Hebrok M. beta-catenin blocks Kras-dependent reprogramming of acini into pancreatic cancer precursor lesions in mice. *J Clin Invest*. 2010 Feb;120:508–20.
9. Zhu LQ, Shi GL, Schmidt CM, Hruban RH, Konieczny SF. Acinar cells contribute to the molecular heterogeneity of pancreatic intraepithelial neoplasia. *Am J Pathol*. 2007 Jul;171:263–73.
10. Lowenfels AB, Maisonneuve P, Cavallini G, Ammann RW, Lankisch PG, Andersen JR, et al. Pancreatitis and the Risk of Pancreatic-Cancer. *N Engl J Med*. 1993 May 20;328:1433–7.
11. Feldmann G, Beaty R, Hruban RH, Maitra A. Molecular genetics of pancreatic intraepithelial neoplasia. *J Hepatobiliary Pancreat Surg*. 2007;14:224–32.
12. Kanda M, Matthaei H, Wu J, Hong SM, Yu J, Borges M, et al. Presence of Somatic Mutations in Most Early-Stage Pancreatic Intraepithelial Neoplasia. *Gastroenterology*. 2012 Apr;142:730–U129.
13. Hruban RH, Goggins M, Parsons J, Kern SE. Progression model for pancreatic cancer. *Clin Cancer Res*. 2000 Aug;6:2969–72.
14. Caldas C, Kern SE. K-Ras Mutation and Pancreatic Adenocarcinoma - State-of-the-Art. *Int J Pancreatol*. 1995 Aug;18:1–6.
15. Maitra A, Hruban RH. Pancreatic cancer. *Annu Rev Pathol-Mech Dis*. 2008;3:157–88.
16. Carriere C, Young AL, Gunn JR, Longnecker DS, Korc M. Acute pancreatitis markedly accelerates pancreatic cancer progression in mice expressing oncogenic Kras. *Biochem Biophys Res Commun*. 2009 May 8;382:561–5.

17. Guerra C, Schuhmacher AJ, Canamero M, Grippo PJ, Verdaguer L, Perez-Gallego L, et al. Chronic pancreatitis is essential for induction of pancreatic ductal adenocarcinoma by k-Ras Oncogenes in adult mice. *Cancer Cell*. 2007 Mar;11:291–302.
18. Morris JP, Wang SC, Hebrok M. KRAS, Hedgehog, Wnt and the twisted developmental biology of pancreatic ductal adenocarcinoma. *Nat Rev Cancer*. 2010 Oct;10:683–95.
19. Kopp JL, von Figura G, Mayes E, Liu F-F, Dubois CL, Morris JP, et al. Identification of Sox9-Dependent Acinar-to-Ductal Reprogramming as the Principal Mechanism for Initiation of Pancreatic Ductal Adenocarcinoma. *Cancer Cell*. 2012 Dec 11;22(6):737–50.
20. Pinho AV, Rooman I, Reichert M, De Medts N, Bouwens L, Rustgi AK, et al. Adult pancreatic acinar cells dedifferentiate to an embryonic progenitor phenotype with concomitant activation of a senescence programme that is present in chronic pancreatitis. *Gut*. 2011 Jul;60:958–66.
21. Rooman I, Real FX. Pancreatic ductal adenocarcinoma and acinar cells: a matter of differentiation and development? *Gut*. 2012 Mar;61:449–58.
22. Bockman DE, Guo JC, Buchler P, Muller MW, Bergmann F, Friess H. Origin and development of the precursor lesions in experimental pancreatic cancer in rats. *Lab Invest*. 2003 Jun;83:853–9.
23. Scarpelli DG, Rao MS, Reddy JK. Studies of Pancreatic Carcinogenesis in Different Animal-Models. *Env Heal Perspect*. 1984;56:219–27.
24. Wagner M, Luhrs H, Kloppel G, Adler G, Schmid RM. Malignant transformation of duct-like cells originating from acini in transforming growth factor a transgenic mice. *Gastroenterology*. 1998 Nov;115:1254–62.
25. Sandgren EP, Quaife CJ, Paulovich AG, Palmiter RD, Brinster RL. Pancreatic Tumor Pathogenesis Reflects the Causative Genetic Lesion. *Proc Natl Acad Sci U S*. 1991 Jan;88:93–7.
26. Hingorani SR, Petricoin EF, Maitra A, Rajapakse V, King C, Jacobetz MA, et al. Preinvasive and invasive ductal pancreatic cancer and its early detection in the mouse. *Cancer Cell*. 2003 Dec;4:437–50.
27. Bardeesy N, Sharpless NE. RAS unplugged: Negative feedback and oncogene-induced senescence. *Cancer Cell*. 2006 Dec;10:451–3.
28. Guerra C, Barbacid M. Genetically engineered mouse models of pancreatic adenocarcinoma. *Mol Oncol*. 2013 Apr;7:232–47.
29. Hingorani SR, Wang LF, Multani AS, Combs C, Deramaudt TB, Hruban RH, et al. Trp53(R172H) and KraS(G12D) cooperate to promote chromosomal instability and widely metastatic pancreatic ductal adenocarcinoma in mice. *Cancer Cell*. 2005 May;7:469–83.
30. Biankin AV, Waddell N, Kassahn KS, Gingras MC, Muthuswamy LB, Johns AL, et al. Pancreatic cancer genomes reveal aberrations in axon guidance pathway genes. *Nature*. 2012 Nov 15;491:399–405.
31. Franceschini A, Szklarczyk D, Frankild S, Kuhn M, Simonovic M, Roth A, et al. STRING v9.1: protein-protein interaction networks, with increased coverage and integration. *Nucleic Acids Res*. 2013 Jan;41:D808–D815.
32. Kondratov RV, Antoch MP. Circadian proteins in the regulation of cell cycle and genotoxic stress responses. *Trends Cell Biol*. 2007 Jul;17:311–7.

33. Gotter AL, Manganaro T, Weaver DR, Kolakowski LF, Possidente B, Sriram S, et al. A time-less function for mouse Timeless. *Nat Neurosci.* 2000 Aug;3:755–6.
34. Chan RC, Chan A, Jeon M, Wu TF, Pasqualone D, Rougvie AE, et al. Chromosome cohesion is regulated by a clock gene paralogue TIM-1. *Nature.* 2003 Jun 26;423:1002–9.
35. Davis S, Mirick DK, Stevens RG. Night Shift Work, Light at Night, and Risk of Breast Cancer. *J Natl Cancer Inst.* 2001 Oct 17;93:1557–62.
36. Kemp MG, Akan Z, Yilmaz S, Grillo M, Smith-Roe SL, Kang T-H, et al. Tipin-Replication Protein A Interaction Mediates Chk1 Phosphorylation by ATR in Response to Genotoxic Stress. *J Biol Chem.* 2010 May 28;285(22):16562–71.
37. Nguyen N, Judd LM, Kalantzis A, Whittle B, Giraud AS, van Driel IR. Random mutagenesis of the mouse genome: a strategy for discovering gene function and the molecular basis of disease. *Am J Physiol Gastrointest Liver Physiol.* 2011 Jan;300:G1–11.
38. Noveroske JK, Weber JS, Justice MJ. The mutagenic action of N-ethyl-N-nitrosourea in the mouse. *Mamm Genome.* 2000 Jul;11:478–83.
39. Takahasi KR, Sakuraba Y, Gondo Y. Mutational pattern and frequency of induced nucleotide changes in mouse ENU mutagenesis. *Bmc Mol Biol [Internet].* 2007 Jun 20;8. Available from: [://000248094500001](http://000248094500001)
40. Andrews TD, Whittle B, Field MA, Balakishnan B, Zhang Y, Shao Y, et al. Massively parallel sequencing of the mouse exome to accurately identify rare, induced mutations: an immediate source for thousands of new mouse models. *Open Biol [Internet].* 2012 May;2. Available from: [://000307112900001](http://000307112900001)
41. Nelms KA, Goodnow CC. Genome-wide ENU mutagenesis to reveal immune regulators. *Immunity.* 2001 Sep;15:409–18.
42. Giry-Laterriere M, Cherpin O, Kim YS, Jensen J, Salmon P. Polyswitch Lentivectors: “All-in-One” Lentiviral Vectors for Drug-Inducible Gene Expression, Live Selection, and Recombination Cloning. *Hum Gene Ther.* 2011 Oct;22:1255–67.
43. Shin K-J, Wall EA, Zavzavadjian JR, Santat LA, Liu J, Hwang J-I, et al. A single lentiviral vector platform for microRNA-based conditional RNA interference and coordinated transgene expression. *Proc Natl Acad Sci.* 2006 Sep 12;103:13759–64.
44. Ornitz DM, Palmiter RD, Messing A, Hammer RE, Pinkert CA, Brinster RL. Elastase I promoter directs expression of human growth hormone and SV40 T antigen genes to pancreatic acinar cells in transgenic mice. *Cold Spring Harb Symp Quant Biol.* 1985;50:399–409.
45. Zhang Y. I-TASSER server for protein 3D structure prediction. *BMC Bioinformatics.* 2008;9:40.
46. Roy A, Kucukural A, Zhang Y. I-TASSER: a unified platform for automated protein structure and function prediction. *Nat Protoc.* 2010;5:725–38.
47. Cerami E, Gao J, Dogrusoz U, Gross BE, Sumer SO, Aksoy BA, et al. The cBio cancer genomics portal: an open platform for exploring multidimensional cancer genomics data. *Cancer Discov.* 2012 May;2:401–4.
48. Adzhubei IA, Schmidt S, Peshkin L, Ramensky VE, Gerasimova A, Bork P, et al. A method and server for predicting damaging missense mutations. *Nat Methods.* 2010 Apr;7:248–9.

49. Jones S, Zhang XS, Parsons DW, Lin JCH, Leary RJ, Angenendt P, et al. Core signaling pathways in human pancreatic cancers revealed by global genomic analyses. *Science*. 2008 Sep 26;321:1801–6.
50. Potter LR. Guanylyl cyclase structure, function and regulation. *Cell Signal*. 2011 Dec;23(12):1921–6.
51. Pitari GM, Di Guglielmo MD, Park J, Schulz S, Waldman SA. Guanylyl cyclase C agonists regulate progression through the cell cycle of human colon carcinoma cells. *Proc Natl Acad Sci*. 2001 Jul 3;98(14):7846–51.
52. Delous M, Yin C, Shin D, Ninov N, Debrito Carten J, Pan L, et al. *sox9b* Is a Key Regulator of Pancreaticobiliary Ductal System Development. *PLoS Genet*. 2012 Jun 14;8(6):e1002754.
53. Manfroid I, Ghaye A, Naye F, Detry N, Palm S, Pan L, et al. Zebrafish *sox9b* is crucial for hepatopancreatic duct development and pancreatic endocrine cell regeneration. *Dev Biol*. 2012 Jun 15;366(2):268–78.
54. Shi G, Zhu L, Sun Y, Bettencourt R, Damsz B, Hruban RH, et al. Loss of the Acinar-Restricted Transcription Factor *Mist1* Accelerates *Kras*-Induced Pancreatic Intraepithelial Neoplasia. *Gastroenterology*. 2009 Apr 1;136(4):1368–78.

## 8. Abbreviations

### **A**

ADM	acinar to ductal metaplasia
Amy2	Amylase 2
ANU	Australian National University
APF	Australian Phenomics Facility
Arf-p53	alternate reading frame of the INK4a/ARF locus
ATR	Ataxia Telangiectasia And Rad3 Related

### **B**

BCA	bicinchoninic acid
BMAL1	Aryl Hydrocarbon Receptor Nuclear Translocator-Like
BSA	Bovine serum albumin
BSD	Blasticidin S hydrochloride

### **C**

cDNA	copy DNA
CHK1	Checkpoint Kinase 1
CLOCK	Clock Circadian Regulator
CNV	copy number variant
Cpa1	carboxypeptidase 1
Ctrb	chymotrypsinogen 1

### **D**

DAB	3,3'diaminobenzidine
DAPI	4',6-diamidino-2-phenylindole
DNA	Deoxyribonucleic acid
dNTP	Deoxyribonucleotide triphosphate
dox	doxycycline hyclate

### **E**

EDTA	Ethylenediaminetetraacetic acid
Ela1	Elastase 1
EMT	epithelial to mesenchymal transition
ENU	N-ethyl-N-nitrosourea

### **F**

FBS	Fetal bovine serum
Fbxw5	F-box and WD repeat domain containing 5
Forw	forward

### **G**

GUCD1	Human Guanylyl cyclase containing domain 1 gene
Gucd1	Mouse Guanylyl cyclase containing domain 1 gene

---

GUCD1	Human Guanylyl cyclase containing domain 1 protein
Gucd1	Mouse Guanylyl cyclase containing domain 1 protein
GUCD1-HA	HA-tagged GUCD1

**H**

H&E	heamatoxylin and eosin
HA	hemagglutinin
HBSS	Hanks balanced salt solution
Hes1	hairy and enhancer of split 1
Het	heterozygous
Hom	homozygous
Hprt	hypoxanthine phosphoribosyltransferase 1
HRP	Horseradish peroxidase

**I**

ICGC	International Cancer Genome Consortium
IF	immunofluorescence
IHC	immunohistochemistry
Ink4a-Rb	Cyclin-Dependent Kinase Inhibitor 2A-retinoblastoma
IPMN	Intraductal papillary mucinous neoplasm

**K**

KPC	Pdx1-Cre; K-Ras <sup>+/LSLG12D</sup> ; p53 <sup>R172H/+</sup>
Kras	V-Ki-Ras2 Kirsten Rat Sarcoma Viral Oncogene Homolog
Krt19	cytokeratin 19
Krt7	cytokeratin 7

**M**

MCN	Mucinous Cystic Neoplasm
MES	2-(N-morpholino)ethanesulfonic acid
Mist1	Muscle, Intestine And Stomach Expression 1
MOPS	3-(N-morpholino)propanesulfonic acid
mRNA	messenger ribonucleic acid

**N**

NaCl	sodium chloride
NGS	next gen sequencing
NPAS2	neuronal PAS domain protein 2
N/A	not assigned

**P**

PanIN	Pancreatic intra-epithelial neoplasia
PDAC	Pancreatic ductal adenocarcinoma
Pdx1	Pancreatic And Duodenal Homeobox 1
PER1	period circadian clock 1
PI3K	Phosphatidylinositol 3-kinase

---

Ppargc1a	peroxisome proliferator-activated receptor gamma, coactivator 1 alpha
Ptf1a	pancreas specific transcription factor, 1a
PVDF	polyvinylidene fluoride
<b>R</b>	
RAF-MAPK	V-Raf Murine Sarcoma 3611 Viral Oncogene Homolog 1-Mitogen-activated protein kinase
RalGDS	Ral Guanine Nucleotide Dissociation Stimulator
Rbpjl	Recombination Signal Binding Protein For Immunoglobulin Kappa J Region-Like
Rev	reverse
RT-qPCR	real time-quantitative polymerase chain reaction
Room temperature	RT
<b>S</b>	
SDS-Page	sodium dodecyl sulfate polyacrylamide gel electrophoresis
Smad4	Mothers against decapentaplegic homolog 4
SNV	single nucleotide variant
Sox9	Sex-Determining Region Y-Box 9
<b>T</b>	
Tbc1d20	TBC1 Domain Family, Member 20
TCGA	The Cancer Genome Atlas
TIM	Human timeless gene
Tim	Mouse timeless gene
TIM	Human timeless protein
Tim	Mouse timeless protein
TIPIN	TIMELESS interacting protein
Tris-HCl	tris(hydroxymethyl)aminomethane-hydrochloride
<b>V</b>	
Vim	vimetin
vs	versus
<b>w</b>	
WB	Western Blot
wp	whole pancreas
<b>Z</b>	
Zfp316	zinc finger protein 316

## 9. Acknowledgements and CV

I wish to thank all the people of the Pancreatic Cancer group but most of all I would first acknowledge the state-of-the-art tutoring I had the pleasure of receiving from my promotor Ilse and supervisors: Amanda, Andreia, Jess and Marc. Furthermore I wish to thank the whole Pancreatic Cancer group, a lot of people from The Kinghorn Cancer Centre but also the Garvan Institute for Medical Research for their help, support and kindness.

A short list of people I thank for their effort in the lab:

Robert Shearer

Mary Iconomou

Ruth Lyons

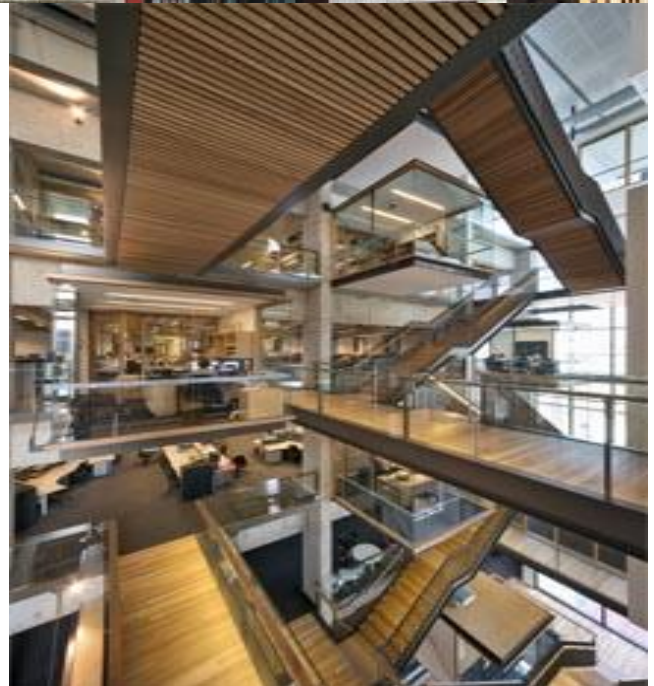
Gillian Lehrbach

Marcelo Sergio

Anita Ledger

Anaïs Zaratzian

Alice Boulgherian



# Curriculum Vitae

Mathias Van Bulck

## Personalialia

Name: Mathias Van Bulck  
 Adres: Nieuwstraat 128  
 Postal code + city: 2840 Terhagen  
 Tel: +323888 43 43  
 Mobile: +32476 973 918 or +61410 994 483  
 E-mail: [mybulck@gmail.com](mailto:mybulck@gmail.com)  
 Date of birth: 15/02/90  
 Place of birth: Antwerp  
 Nationality: Belgian  
 Drivers license: No  
 Marital status: unmarried  
 sofi-number: 484210054

## Education

2002-2008	ASO science-mathematiques - completed with distinction	St-Ritacollege Kontich, BEL
2008-2011	BSc in biomedical sciences(with distinction) - Completed with distinction	Vrije universiteit Brussel(VUB), BEL
2011	Bachelor thesis: 'A cellular energy sensor with possible role in diabetes'	Vrije universiteit Brussel(VUB), BEL
2011-2013	MSc in biomedical sciences	Vrije universiteit Brussel(VUB), BEL
2013	Master thesis: 'ENU mutagenesis as a discovery and validation tool of potential driver genes in pancreatic tumourigenesis'	The Garvan Institute of Medical Research, Sydney NSW, AUS

## Internships and job experience

2011	Studentjob at AML (department of molecular biology)	Antwerp, BEL
2012-2013	3-month internship at the Centre of Medical Genetics	University hospital Brussels, BEL

3-month internship at the Laboratory of Medical and Molecular Oncology	University hospital Brussels, BEL
8-month internship at the Pancreatic Cancer Group, Cancer Research Program, The Garvan Institute of Medical Research/The Kinghorn Cancer Centre	The Garvan Institute of Medical Research, Sydney NSW, AUS

### Extracurricular development

2011	15th Maastricht medical students research conference	Maastricht University, Maastricht, NED
2012	6th Garvan signalling symposium	The Garvan Institute of Medical Research, Sydney NSW, AUS
2013	Sydney catalyst: Post-graduate student and early-career researcher symposium	The Garvan Institute of Medical Research, Sydney NSW, AUS
	Jalview workshop	The Garvan Institute of Medical Research, Sydney NSW, AUS
	4th annual Australian Pancreatic Genome Initiative meeting	The Garvan Institute of Medical Research, Sydney NSW, AUS
	MOSA conference: International students research conference on health. Winner student science prize for best poster presentation.	Maastricht University, Maastricht, NED

### Miscellaneous

2007	Student job at Wienerberger building material solutions	Rumst, BEL
2008-2011	Monitor archery summer camps	Oordegem, BEL

2009	BLOSO Trainer A certification	Antwerp, BEL
2010	International Youth Judge certification by World Archery	Shanghai, CHN
2011	Participant World Archery management seminar	Lausanne, SUI
2013	KSL International Archery Coach: level 1 certification by KSL International Archery	Sydney, AUS

### IT-knowledge

---

MS Word	Extensive
MS excel	Extensive
MS powerpoint	Extensive
OO writer	Extensive
OO impress	Sufficient
OO calc	Sufficient
Vector NTI	Sufficient
Alamut	Sufficient
Adobe Photoshop	Sufficient
ImageJ	Extensive
SDS 2.4	Extensive
Prism 6.0	Extensive

### Languages

---

Dutch	Native language
English	Very good
French	Very good
German	basic